AGU ADVANCING EARTH AND SPACE SCIENCES

Tectonics

RESEARCH ARTICLE
10.1029/2024TC008362

Machine Learning-Based Spatio-Temporal Prospectivity Modeling of Porphyry Systems in the New Guinea and Solomon Islands Region

Ehsan Farahbakhsh[1], **Sabin Zahirovic**[1], **Brent McInnes**[2], **Sara Polanco**[1,3], **Fabian Kohlmann**[4], **Maria Seton**[1], **and R. Dietmar Müller**[1]

[1]EarthByte Group, School of Geosciences, The University of Sydney, Sydney, NSW, Australia, [2]John de Laeter Centre, Faculty of Science and Engineering, Curtin University, Perth, WA, Australia, [3]School of Environmental and Life Sciences, University of Newcastle, Callaghan, NSW, Australia, [4]Lithodat Pty. Ltd., Melbourne, VIC, Australia

Key Points:

- Machine learning models link porphyry system formation to subduction zone evolution, offering new exploration insights
- Key factors like seafloor spreading and convergence rates and subduction obliquity significantly influence porphyry mineralization potential
- Oblique subduction and elevated convergence rate increase the likelihood of mineralization in the New Guinea and Solomon Islands region

Supporting Information:

Supporting Information may be found in the online version of this article.

Correspondence to:

E. Farahbakhsh,
e.farahbakhsh@sydney.edu.au

Citation:

Farahbakhsh, E., Zahirovic, S., McInnes, B., Polanco, S., Kohlmann, F., Seton, M., & Müller, R. D. (2025). Machine learning-based spatio-temporal prospectivity modeling of porphyry systems in the New Guinea and Solomon Islands region. *Tectonics*, *44*, e2024TC008362. https://doi.org/10.1029/2024TC008362

Received 16 APR 2024
Accepted 19 FEB 2025
Corrected 24 MAR 2025

This article was corrected on 24 MAR 2025. See the end of the full text for details.

Abstract

The discovery of new economic copper deposits is critical for the development of renewable energy infrastructure and zero-emissions transport. The majority of existing copper mines are located within current or extinct continental arc systems, but our understanding of the tectonic and geodynamic conditions favoring the formation of porphyry systems is still incomplete. Traditionally, exploration criteria are based on present-day geological and geophysical observations rather than the time-dependent evolution of subduction systems. Addressing this knowledge gap, our study connects the formation of porphyry systems, particularly enriched in copper, with subduction zone evolution, utilizing machine learning in a spatio-temporal mineral prospectivity framework. Incorporating Cenozoic intrusion-related copper-gold deposits in the New Guinea and Solomon Islands region, we develop a model that accurately predicts known mineral occurrences and identifies key features for potential porphyry mineralization in the study area. Key findings include the importance of the obliquity angle of subduction, which significantly affects strain partitioning, crustal fluid flow, and ore deposition, with angles between 10 and 50° favored for mineralization. Furthermore, rapid plate convergence and seafloor spreading half-rates ranging from 30 to 45 mm/yr potentially enhance mineralization prospects by promoting metasomatism and hydrous melting. This approach, integrating plate motion models with machine learning, provides new exploration criteria, enhancing our understanding of porphyry ore formation mechanisms and guiding future exploration in both active and abandoned subduction zones.

Plain Language Summary

Copper is essential for renewable energy systems and electric vehicles, making the discovery of new copper sources critical. Most existing copper mines are located in regions where Earth's tectonic plates interact, but we do not fully understand why some areas have rich copper deposits while others do not. Traditional methods of finding copper focus on current geological features without considering how Earth's surface has changed over time. Our study explores how the movement of tectonic plates affects the formation of copper-rich deposits. We use machine learning to analyze data across both time and space. Specifically, we look at the New Guinea and Solomon Islands region known for copper and gold deposits. Our model accurately predicts where copper deposits are found and highlights key factors that contribute to their formation. We discover that the angle at which one tectonic plate moves under another called the subduction angle, plays a significant role. Angles between 10 and 50° are most favorable for creating copper deposits. Additionally, faster movement of the plates and certain rates of new seafloor formation increase the chances of finding copper. This new approach provides valuable guidelines for exploring copper deposits and enhances our understanding of how they form.

1. Introduction

Exploring for new supplies of copper is vital for the energy transition because of its exceptional electrical conductivity (Church & Crawford, 2020) and its essential use in the manufacture of electric vehicles, renewable energy infrastructure, and energy storage systems (Jowitt & McNulty, 2021). The role of copper in electricity transmission and its use in batteries contributes to sustainability goals, making it a key element in advancing technologies for a cleaner and more sustainable energy future (Larcher & Tarascon, 2015). Copper is mainly derived from porphyry ore deposits, characterized by low-grade and high-tonnage mineralization (Park et al., 2021). Despite their relatively low copper grade, the sheer volume of porphyry deposits and frequently easy accessibility close to the surface makes them high prospectivity targets and pivotal in meeting future global copper demand (Park et al., 2021).

The last decades of the 20th century witnessed remarkable advancements in ore deposit discoveries attributed to the evolution of geophysical and geochemical surface detection techniques (Wood & Hedenquist, 2019); however, the discovery rates of easily accessible near-surface deposits have markedly declined (Mudd & Jowitt, 2018; Wood & Hedenquist, 2019). Searching deeper into the crustal profile necessitates the deployment of advanced and costly exploration technologies (Cooke et al., 2020; Nathwani et al., 2023) and the integration of geological, geochemical, and geophysical data sets. These integration methods, which may be limited by potentially incomplete data sets in frontier greenfield areas (Farahbakhsh et al., 2023; Sun et al., 2019), may be augmented by spatio-temporal modeling workflows. These spatio-temporal workflows utilize advanced statistical and machine learning techniques that incorporate temporal changes in plate motion models into copper prospectivity assessments (Butterworth et al., 2016; Diaz-Rodriguez et al., 2021). This approach simulates subduction regimes and establishes favorable settings in both space and time for the formation of porphyry ore systems. Changes in subduction regimes are often viewed as critical factors triggering mineralization events, such as those linked to terrane collisions, subduction of slab structures, or variations in slab angle during subduction (Cooke et al., 2005; J. P. Richards, 2013; S. W. Richards & Holm, 2013; Rosenbaum & Mo, 2011; Rosenbaum et al., 2005; Sillitoe, 2010). A comprehensive understanding of the geological contexts associated with deposit emplacement becomes essential as mineral exploration advances to target concealed deposits beneath cover. Spatio-temporal models can be combined with conventional exploration targeting methods to de-risk exploration using a plate motion paradigm.

The established association between porphyry ore deposits and subduction has brought attention to the poorly understood subduction parameters that primarily influence the genesis of these deposits (Cooke et al., 2005; J. P. Richards, 2013). The intricate interplay of specific geodynamic parameters, influencing the coupling between the downgoing and overriding plates, plays a pivotal role in determining and controlling the types of magmatism and subsequent ore formation in subduction arcs. Currently, no singular parameter has been identified as a primary determinant of arc magmatism, suggesting a dynamic interplay among multiple conditions governing tectonic regime, magmatism, and porphyry copper genesis. Butterworth et al. (2016) proposed a comprehensive four-dimensional approach, integrating machine learning, ore deposit geochronology, and plate tectonic modeling to identify key predictors for Andean porphyry copper magmatism. They highlighted that parameters such as convergence rate, subduction obliquity, subducting oceanic crust age, and distance from trench lines influence porphyry magmatism in South America and linked these observations to total and carbonate oceanic sediment thickness, small-scale convection, and the presence of partial melt in the mantle wedge. Building on this, Diaz-Rodriguez et al. (2021) linked slab properties and orthogonal plate convergence velocities to continental arc thickening, material transport, and metasomatic enrichment of the mantle wedge to porphyry copper genesis across the Americas' active margins. Also, in a recent study on the same region, Alfonso et al. (2024) identified thick arc crust, rapid convergence, and a sufficient supply of volatile fluids into the subduction system as the primary prerequisites for mineralization.

In this study, we incorporate recent advances in the understanding of Asia-Pacific plate motions over the last 30 million years into a new spatio-temporal data analysis approach, building on previous advances (Butterworth et al., 2016; Diaz-Rodriguez et al., 2021), to investigate the genesis of porphyry systems in the New Guinea and Solomon Islands region. This region is renowned for its wealth of relatively young porphyry deposits. These deposits provide unique insights into the geological processes at play, thanks to our clearer understanding of their kinematics. This knowledge contrasts sharply with that of older deposits, where much of the geological record has been obliterated, and uncertainties abound regarding the geological processes driving their formation. Consequently, younger deposits present unparalleled opportunities for studying and predicting the formations of porphyry systems within a dynamic tectonic environment (Holm et al., 2019). Employing robust machine learning methods and benefiting from the recent advances in the field (Farahbakhsh et al., 2023), our goal is to identify the critical tectonic conditions and configurations associated with ore deposit formation and determine where and when episodes of porphyry mineralization may have occurred.

2. Geological Setting

The New Guinea and Solomon Islands region, situated in the southwest Pacific, represents a quintessential example of tectonic complexity and dynamism. This area is characterized by an intricate interplay between the

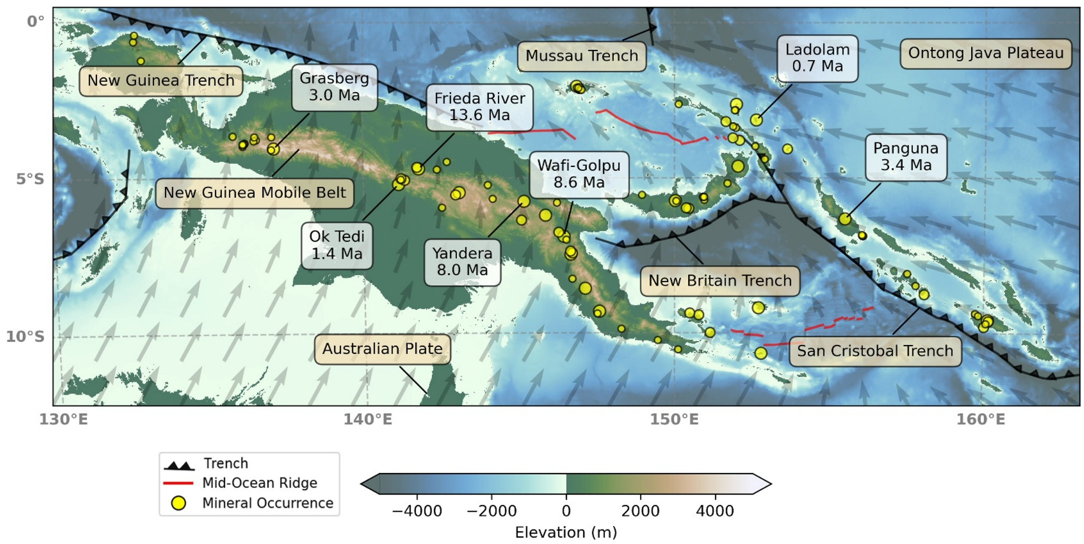

Figure 1. Trench lines in the active subduction zones around New Guinea and the Solomon Islands mapped using the R. D. Müller et al. (2019) model, with plate motion velocity vectors from the plate reconstructions in a mantle reference frame and porphyry occurrences represented by yellow circles sized proportionally to their significance. Some major deposits, along with their formation ages, are shown on the map.

Indo-Australian and Pacific plates, resulting in a convoluted arrangement of active subduction zones, island arcs, and associated crustal deformations that significantly influence its geological and metallogenic evolution (e.g., Crowhurst et al., 2004; Davies, 2012; Hill & Hall, 2003; Holm et al., 2015). As shown in Figure 1, the tectonic framework of this region is defined by several principal units, including the Australian Continental Block, the New Guinea Mobile Belt, and distinct island arcs such as the northern New Guinea-New Britain Arc and the Admiralty-Solomon Island Arc (Davies, 2012; Hill & Raza, 1999; Holm et al., 2013; Petterson et al., 1999; Woodhead et al., 1998).

The Australian Continental Block, located in the southwest of the study area, is delineated by a Paleozoic crystalline basement overlain by granitic rocks, indicative of ancient continental crust (Craig & Warvakai, 2009; Hill & Gleadow, 1989). In contrast, the New Guinea Mobile Belt, which borders the Australian Continental Block to the north and east, emerges as a zone of interaction between the colliding Indo-Australian and Pacific plates (Davies, 2012; Hill & Raza, 1999). This mobile belt is replete with major and thrust faults, alongside a variety of intrusive and metamorphic rocks predominantly of Mesozoic to recent ages, reflecting ongoing tectonic activity and crustal dynamics (Abbott, 1995; Hall, 2002; Holm et al., 2016).

The collision of these tectonic plates not only fosters the formation of the complex series of island arcs but also drives significant geological processes, including uplift, deformation, and magmatism (e.g., Crowhurst et al., 2004; Davies, 2012; Hill & Hall, 2003; Holm et al., 2015; Zahirovic et al., 2016). These processes are evidenced by rapid plate movements, with rates up to 100 mm per year, leading to considerable crustal accretion and shortening, thereby sculpting distinctive geological terranes of the region, such as the Australian Continental Block, the New Guinea Orogen, and the New Guinea Islands Terrane (Hill & Hall, 2003; Tregoning et al., 2000). Each terrane exhibits a unique assembly of rock types, structures, and mineral potentials, contributing to the geological diversity of the region.

The tectonic evolution of this region is further complicated by collision events such as the Ontong Java Plateau with the Solomon Islands and the subsequent collision of the Australian continent with Papua New Guinea (Holm et al., 2019). These collisions have been instrumental in shaping the metallogenic profile of the area, facilitating the formation of gold-rich deposits and porphyry copper occurrences (Figure 1), such as Grasberg, Frieda River, Panguna, Wafi-Golpu, and Ok Tedi (Cooke et al., 2005; Holm et al., 2019; J. P. Richards, 2013; Sillitoe, 2010), through various mechanisms including the tearing of subducted slabs, development of slab windows, and upper plate deformations that enhance magma flux from the mantle (e.g., Cooke et al., 2005; J. P. Richards, 2013; S. W. Richards & Holm, 2013; Sillitoe, 2010). The New Guinea and Solomon Islands region serves as an exemplary model for understanding complex convergent margins. The geodynamic settings of the region, characterized by a myriad of tectonic interactions, subduction dynamics, and magmatic activities, play a pivotal role in its mineralization processes and prospectivity. Recognizing the multifaceted tectonic and geological intricacies of this region not only aids in unraveling its geological history but also in refining exploration models and strategies for mineral resource development.

3. Genetic Model

Porphyry copper systems, along with other ore-bearing systems like polymetallic sulfide and epithermal gold deposits, originate in magmatic arcs located along subduction zones within convergent margins (J. P. Richards, 2003; Sillitoe, 1972, 2010). These systems are typically found in linear, orogen-parallel belts corresponding to their associated magmatic arcs, which are usually active for periods ranging between 10 and 20 million years (Sillitoe, 2010). Porphyry systems in post-collisional settings can also be formed, linked to mildly alkaline and sulfur-poor magmas resulting from remelting previously subducted arc lithosphere (J. P. Richards, 2009). However, these systems are not tied to ongoing and contemporaneous subduction processes. The mechanisms responsible for generating porphyry systems fall into two categories: conditions within subduction zones related to the interaction between the downgoing and overriding plates and geological processes occurring in the overlying asthenospheric mantle wedge, subcontinental mantle lithosphere, and continental crust. The first category is influenced by the tectonic setting that defines the frictional coupling between the subducting and overriding plates. Factors controlling this setting include the tectonic regime, which can range from moderately extensional to compressional, including oblique slip regimes that, when transmitted into the overriding plate, result in contraction and/or extension, as well as shear strains that generate strike-slip or pull-apart structural frameworks (J. P. Richards, 2003; Sillitoe, 2010; Tosdal & Richards, 2001). The stress regimes are primarily determined by whether the trench is advancing or rolling back.

The regional stress regimes are also influenced by various factors, including the obliquity of the subducting convergence, the velocity, dip, and buoyancy of the subducting slab—largely governed by its age and temperature—and the subduction of distinctive seafloor features such as ridges and seamounts (J. P. Richards, 2003). Additionally, the tearing of the subducting slab plays a role in determining stress regimes (D. Müller et al., 2002). The second set of mechanisms involves the impact on the descending plate due to dehydration occurring at depths around 100 km, coinciding with the blueschist-eclogite transition. During this phase, the asthenospheric mantle resembling mid-ocean ridge basalt undergoes metasomatism, resulting in an enrichment of volatiles, sulfur, silica, and fluid-mobile large ion lithophile elements (J. P. Richards, 2003). Adiabatic decompression melting of this metasomatized mantle material leads to the production of ascending hydrous and oxidized mafic magmas (D. Müller et al., 2002; J. P. Richards, 2014). These magmas ascend from the upper mantle and accumulate in crustal magma chambers.

The fractionation of these magma chambers can release pulses of fertile melt rising from the cupolas of the chambers into the upper crust, where they have the potential to form porphyry deposits (J. P. Richards, 2003, 2014). The generation of porphyry deposits is also influenced by factors such as magmatic water content, magma oxidation state, and sulfur saturation (Park et al., 2021; J. P. Richards, 2014). Recent studies have expanded our understanding of porphyry deposit formation, emphasizing the critical role of magma dynamics and crustal conditions. Chiaradia and Caricchi (2022) propose that supergiant porphyry copper deposits may represent "failed large eruptions," where rapid magma injection rates and specific crustal thicknesses lead to magma storage rather than eruption, facilitating mineralization. Similarly, Lee and Tang (2020) highlight the importance of neutral buoyancy levels in determining whether magma ascends to erupt or stalls to form porphyry systems. These insights suggest that the interplay between magma injection rates, crustal thickness, and buoyancy levels is crucial in dictating the dual pathways of eruption versus mineralization in porphyry systems. Incorporating these factors into prospectivity modeling could enhance predictions of porphyry deposit locations.

4. Materials and Methods

4.1. Mineral Occurrences

This study utilizes data from 96 Cenozoic copper-gold deposits related to subduction arc evolution and intrusion-related mineralization, including operational mines and exploration prospects, compiled by Hammarstrom et al. (2013) and Holm et al. (2019). This data set, available as Supporting Information S1, encompasses information on the type of deposit, major commodities, tonnage, and the concentration of copper, gold, and molybdenum calculated from both corporate reports and prior studies (see Hammarstrom et al. (2013) and Holm et al. (2019) for further details). The deposits, varying from the late Oligocene to the Quaternary, primarily consist of porphyry deposits in mainland New Guinea within the New Guinea Orogen, with notable sites like Grasberg, Ok Tedi, and Porgera (Figure 1). Additionally, both epithermal and porphyry deposits are found along the Papuan Peninsula and into the Woodlark Basin, featuring a mix of copper-rich and gold-rich locations. In the eastern islands and Solomon Islands, mineral deposits of various ages include porphyry, epithermal, and seafloor massive sulfide (SMS) types, with no distinct preference for copper or gold dominance, highlighting significant sites such as the high-grade SMS Solwara and the major Ladolam and Panguna deposits.

4.2. Plate Motion Models and Features

In this study, we perform spatio-temporal modeling by integrating geological data with plate motion models through the application of pyGPlates—a Python module that extends the plate reconstruction functionalities initially introduced in GPlates (R. D. Müller et al., 2018). The plate reconstructions provide valuable insights into the kinematics of subduction across diverse temporal periods. Our approach involves utilizing and comparing two distinct plate motion models presented by R. D. Müller et al. (2016, 2019), both characterized by a temporal resolution of 1 million years. The model proposed by R. D. Müller et al. (2016) adopts a rigid global plate motion perspective, featuring continuously closing plate boundaries from the Triassic period (230 Ma) to the present. This model investigates the impact of subducting plate age profiles on trench rollback and driving forces by incorporating regional plate models. The R. D. Müller et al. (2019) model represents a global Mesozoic–Cenozoic deforming plate motion model, capturing the progressive extension of all continental margins since the inception of rifting within Pangea around 240 Ma. This model also takes into account major failed continental rifts and compressional deformation along collision zones, reconstructing the outlines and timing of regional deformation episodes based on various published tectonic models and associated geological and geophysical data. Notably, in the R. D. Müller et al. (2019) model, absolute plate motions are reconstructed in a mantle reference frame through a joint global inversion process that minimizes global trench migration velocities and ensures accuracy in depicting net lithospheric rotation (Tetley et al., 2019).

Specifically, in regions like Southeast Asia (Sundaland, Proto–South China Sea, and New Guinea) and the eastern Tethys, the R. D. Müller et al. (2016) model seamlessly integrates with the Zahirovic et al. (2014) model. Similarly, the R. D. Müller et al. (2019) model incorporates the Zahirovic et al. (2016) model in the central and eastern Tethys, Eurasia, and New Guinea. The refined model proposed by Zahirovic et al. (2016) notably enhances our understanding of the tectonic evolution in New Guinea compared to its predecessor (Zahirovic et al., 2014), incorporating refined plate reconstructions and numerical geodynamic modeling. This refinement is particularly evident in the New Guinea margin, including adjustments to the Philippine Sea Plate and the Maramuni arc. The revised model provides a more consistent approach to tracking slabs in the mantle, addressing the complexities of subduction history in the Tethys, East and Southeast Asia, and New Guinea. Additionally, the revised model accounts for additional slab volumes above mid-mantle depths, such as the subduction of the Sepik oceanic gateway and the Maramuni arc, occurring during specific time periods. The improvements to plate reconstructions and the inclusion of subduction zones along New Guinea enhance the congruence between predicted slab distributions and mantle structures inferred from seismic tomography. Consequently, this study predominantly focuses on results derived from the R. D. Müller et al. (2019) model, briefly contrasting them with those obtained using the R. D. Müller et al. (2016) model in Supporting Information S1.

Using these models, we reconstruct and trace various point sets, including mineral occurrences from as far back as 30 Ma and trench points along trench lines, from which we can derive kinematic information. To ensure we capture significant porphyry deposits, we select equidistant points along trench lines, maintaining a 0.1-degree separation (Sillitoe, 2010). The analysis of plate kinematic features spans both relative and absolute plate motions. Absolute plate motions are computed by combining relative motions with a reference frame that anchors them to the deep mantle, as detailed by O'Neill et al. (2005). The determination of the absolute motion for both subducting and overriding plates involves calculating the stage rotation between the subducting plate and the mantle. Convergence is then evaluated by examining the relative stage rotations of the overriding and downgoing plates. The positive convergence rate is defined when plates move toward the overriding plate. The obliquity of subduction is established by measuring the angle between the convergence direction and the lateral trench direction at each sampling point. The obliquity angles extend from -90 to 90°, and a 0° angle denotes a subducting plate

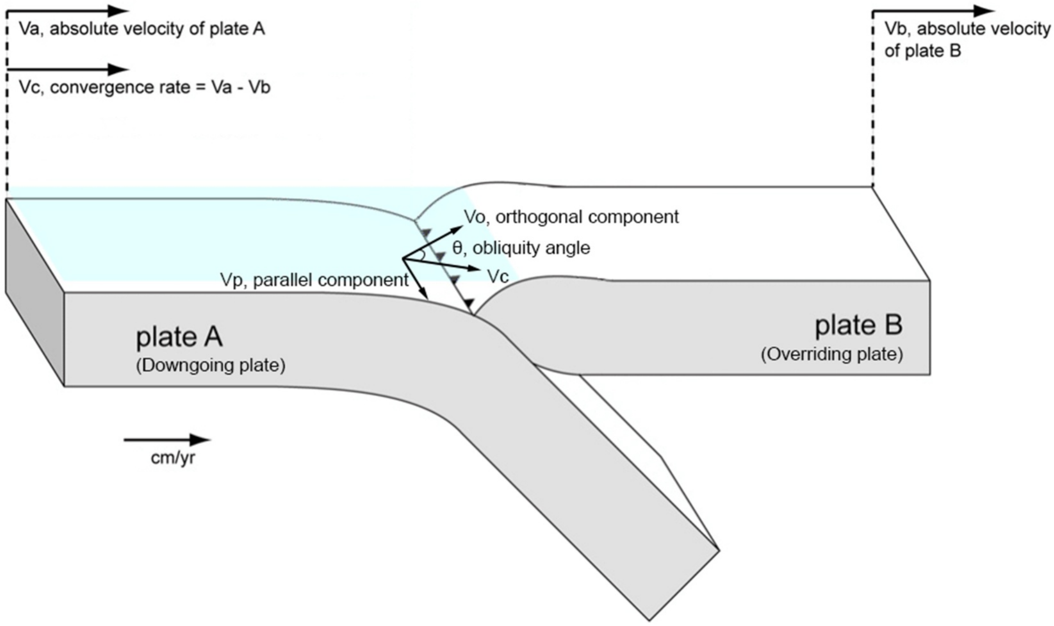

Figure 2. Definition of convergence rate (Vc), considering absolute plate motions (Va and Vb) and obliquity angle (θ). Directions and lengths of arrows are arbitrarily chosen (modified from Bertrand et al. (2014)).

perpendicular to the trench. Angles range clockwise from 0 to 90° as observed from above the Earth, extending from the trench-normal direction to the velocity vector. Conversely, the range from 0 to −90° represents a counter-clockwise progression of angles. The trench normal vector utilized in the obliquity calculations is orthogonal to the great circle arc of each point (arc midpoint) and is directed toward the overriding plate. Our modeling approach encompasses various features, including the magnitude and obliquity angle, along with the parallel and orthogonal components of three velocity vectors. These vectors account for the absolute velocities of both the downgoing and overriding plates, along with the convergence rate indicated by the relative motion vector, calculated over a time interval of 1 million years (Figure 2). Additionally, we incorporate the distance to the nearest trench edge for each trench point, defining the trench edge as the position on the trench line where the subducting or overriding plate changes. The length of the arc segment where each trench point is located is also considered a feature in this study.

We incorporate oceanic paleo-seafloor age grids from both models as an additional feature, shedding light on the coupling dynamics between the downgoing plate and the overriding plate. Our analysis further integrates time-dependent deep-sea carbonate sediment thickness grids, from Dutkiewicz et al. (2018) and R. D. Müller et al. (2022) based on the plate motion models of R. D. Müller et al. (2016, 2019), respectively. These grids model deep-sea carbonate sediment thickness based on global carbonate compensation depth models, carbonate sedimentation rates, and paleobathymetry. Additionally, we leverage grids depicting the percentage of carbon storage in the upper oceanic crust (300 m thick), developed by R. D. Müller and Dutkiewicz (2018) and R. D. Müller et al. (2022) based on the plate motion models of R. D. Müller et al. (2016, 2019), respectively. These grids quantify the proportion of carbon storage in the upper oceanic crust resulting from CO_2 degassing at mid-ocean ridges. Furthermore, we incorporate deep-sea total sediment thickness grids from Dutkiewicz et al. (2017) and R. D. Müller et al. (2022), generated using the plate motion models of R. D. Müller et al. (2016, 2019), respectively. These grids are constructed through a regression algorithm incorporating seafloor age, mean distance to the nearest passive margins, and long-term decompacted sedimentation. Moreover, as a distinctive feature, we compute the subduction volume at each trench point—a function of the orthogonal component of the relative motion vector, the thickness of the subducting plate, and the length of arc segments.

Additionally, seafloor spreading half-rate grids contribute another feature to our workflow. Employing pyGPlates, we create seafloor spreading half-rate grids by first interpolating isochrons (lines of constant age) from the rotation model, ridges, and isochron data provided by R. D. Müller et al. (2016, 2019). These isochrons are then converted into densely spaced points with associated age information. Subsequently, we perform interpolation of

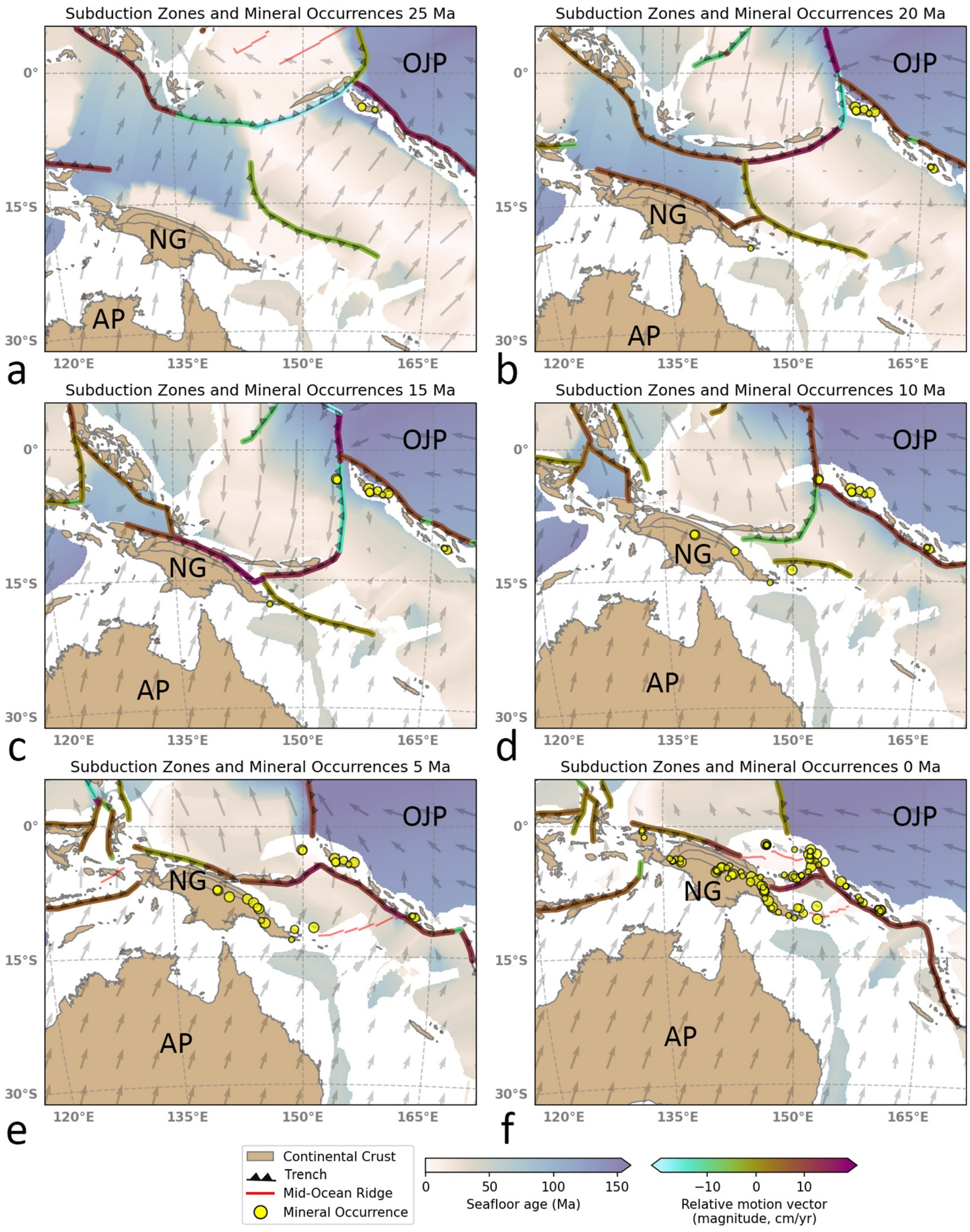

Figure 3. Reconstructed locations of mineral occurrences in New Guinea and the Solomon Islands, modeled from 25 Ma to the present day using the R. D. Müller et al. (2019) model (a–f). Feature values from the closest trench point at the time of each mineral occurrence's formation, within a 3-degree search radius, are assigned to each occurrence. AP, Australian Plate; NG, New Guinea; OJP, Ontong Java Plateau.

the age points onto a global grid, utilizing spherical interpolation to accommodate Earth's curvature. To refine our calculations, we apply a continental block mask grid to the age grid, excluding non-oceanic crust areas from the final computations. Feature generation from the oceanic grids involves calculating the mean pixel values within a circular buffer zone with a radius of 3° around each trench point. This approach allows us to extract information about the characteristics of the surrounding area for each point. Feature values from the nearest trench point within a search radius of 3° are assigned to each sampling point, including mineral occurrences (Figure 3).

Table 1
List of the Features Extracted From the Plate Motion Models and Oceanic Grids at Subduction Zones

			Reference based on the plate motion model	
Feature	Component	Unit	R. D. Müller et al. (2016)	R. D. Müller et al. (2019)
Downgoing absolute plate velocity	Magnitude	cm/yr	R. D. Müller et al. (2016)	R. D. Müller et al. (2019)
	Orthogonal	cm/yr		
	Parallel	cm/yr		
	Obliquity angle	deg		
Overriding absolute plate velocity	Magnitude	cm/yr		
	Orthogonal	cm/yr		
	Parallel	cm/yr		
	Obliquity angle	deg		
Relative motion vector	Magnitude	cm/yr		
	Orthogonal	cm/yr		
	Parallel	cm/yr		
	Obliquity angle	deg		
Deep-sea carbonate sediment thickness	–	m	Dutkiewicz et al. (2018)	R. D. Müller et al. (2022)
Distance to the nearest trench edge	–	deg	R. D. Müller et al. (2016)	R. D. Müller et al. (2019)
Distance to the nearest trench point	–	deg	–	–
Length of the arc segment	–	deg	R. D. Müller et al. (2016)	R. D. Müller et al. (2019)
Seafloor age	–	Ma	R. D. Müller et al. (2016)	R. D. Müller et al. (2019)
Seafloor spreading half-rate	–	mm/yr	–	–
Subducting plate volume	–	km^3/yr	R. D. Müller et al. (2016)	R. D. Müller et al. (2019)
Total deep-sea sediment thickness	–	m	Dutkiewicz et al. (2017)	R. D. Müller et al. (2022)
Upper ocean crust carbonate concentration	–	%	R. D. Müller and Dutkiewicz (2018)	R. D. Müller et al. (2022)

The distance to the nearest trench point is also incorporated as an additional feature. We assume that there is no time lag between the subduction process and the formation of mineral occurrences in the overriding plate. The comprehensive list of features extracted from plate motion models and oceanic grids at subduction zones is presented in Table 1. Furthermore, maps illustrating some of the feature values based on the R. D. Müller et al. (2019) plate motion model along trench lines in the study area for the present day are depicted in Figure 4.

4.3. Machine Learning Framework

In this study, we employ a supervised machine learning framework, specifically focusing on classification—a paradigm where a model is trained on a labeled data set, enabling it to map input data to corresponding output labels under the guidance of a supervisor (Singh et al., 2016). Classification, a common task in supervised learning, entails training a model to assign predefined categories or labels to input data based on patterns learned from the labeled training set, with the labels here denoting mineralized and barren areas (Farahbakhsh et al., 2023). Our framework integrates a series of data processing and machine learning methods to provide a spatio-temporal prospectivity model. A combination of positive and unlabeled bagging (PUB) with random forest serves as the classifier for predicting mineralization zones (Breiman, 2001; Mordelet & Vert, 2014). These methods effectively handle complex and non-linear data, enhancing the recognition of hidden patterns in the quest for a comprehensive spatio-temporal prospectivity model.

In supervised learning, having both positive and negative training samples is crucial for constructing an accurate and reliable model (Singh et al., 2016). In the realm of spatio-temporal prospectivity modeling, these samples serve to train a machine learning model to discern kinematic features associated with mineral occurrences. Positive samples represent areas with known mineral occurrences, while negative samples encompass areas where no mineral occurrences have been identified. Throughout the training process, the model is exposed to both positive and negative samples, enabling it to grasp the kinematic features linked to mineralization. By recognizing

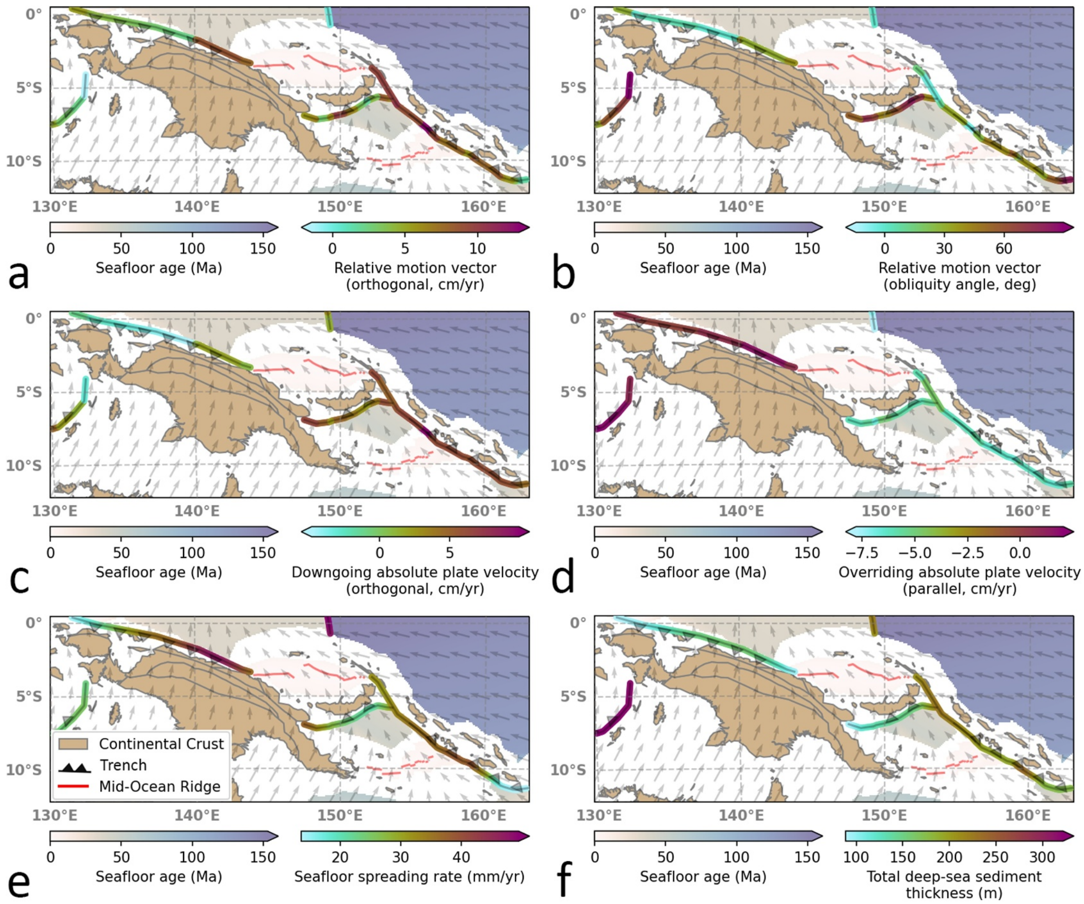

Figure 4. Some of the extracted features including (a) the orthogonal component of the relative motion vector, (b) the obliquity angle of the relative motion vector, (c) the orthogonal component of the downgoing absolute plate velocity, (d) the parallel component of the overriding absolute plate velocity, (e) the seafloor spreading half-rate, and (f) total deep-sea sediment thickness. These features are based on the relative and absolute motion vectors along subduction zones, as well as various oceanic grids surrounding New Guinea and the Solomon Islands, utilizing the R. D. Müller et al. (2019) plate motion model for present-day.

patterns and relationships between these features and established mineral occurrences, the model becomes adept at predicting the likelihood of discovering additional occurrences in different locations. The incorporation of negative samples is particularly pivotal to prevent the model from generating false positives. In the absence of negative samples, the model might erroneously highlight areas devoid of mineral occurrences. By including examples of areas without mineral occurrences, the model can learn to distinguish between locations that are prospective for mineralization and those that are not.

For a meaningful model, the total number of training samples should ideally be at least 10 times the number of features (Farahbakhsh et al., 2023; Figueroa et al., 2012). In our study, we have 96 positive samples or mineral occurrences with 21 features, before excluding highly correlated ones. Consequently, to generate a meaningful model, we require a balanced training data set including a minimum of 105 positive and 105 negative samples. Generating a reliable set of negative samples for mineral prospectivity modeling is a persistent challenge, as these samples, representing areas lacking the target mineralization type, often lack comprehensive and reliable data. Factors such as limited exploration efforts, insufficient geological data, or the presence of masking variables can contribute to the absence of mineral occurrences, making it challenging to precisely define areas devoid of mineral deposits for training machine learning models. In our study, we employ PUB to generate a set of negative samples based on positive samples, aiming to mitigate the challenges associated with creating a robust set of negative samples.

4.3.1. PUB

Different approaches have been proposed for generating negative samples, each carrying its own advantages and drawbacks (e.g., Butterworth et al., 2016; Qi et al., 2005; Zuo & Carranza, 2011). Randomly generating negative samples may introduce undiscovered economic commodities and lead to mislabeling false negatives. Conversely, overly restrictive negative training set selection may result in overfitting and reduced predictive accuracy (Carranza & Laborte, 2016). In recent years, machine learning methods within the positive and unlabeled learning (PUL) category have emerged, requiring positive and unlabeled samples for model training (Mordelet & Vert, 2014). PUL, a semi-supervised binary classification approach, retrieves labels from unknown samples by learning from positive samples (Mordelet & Vert, 2014). This study employs a PUL method known as PUB for labeling unknown samples. PUB, a parallelized bootstrap approach, trains multiple binary classifiers to differentiate known positive examples from random subsamples of the unlabeled set and averages their predictions (Gan et al., 2022; Mordelet & Vert, 2014). Using PUB enables the recovery of labels from unlabeled samples, aiding in the identification of previously unknown mineral occurrences and enhancing the accuracy of predictive models. We uniformly generate an equal number of random samples to known mineral occurrences across the region of interest and time window as depicted in Figure 5 and employ PUB for labeling them. PUB can serve as a wrapper for any supervised learning algorithm, generating reliable positive and negative samples. In this study, it is used to wrap a random forest classifier.

4.3.2. Random Forest

Random forest stands out as a widely used machine learning algorithm with diverse applications, notably in predicting the likelihood of mineralization in unexplored areas (e.g., Farahbakhsh et al., 2023; Sun et al., 2019; Zhang et al., 2022). Functioning as an ensemble learning method, it amalgamates multiple decision trees to fashion a more accurate and resilient model (Breiman, 2001). This supervised learning algorithm is versatile, adept at handling both classification and regression problems, and is celebrated for its user-friendly nature, minimal data pre-processing requirements, and capability to manage missing values. The algorithm generates numerous decision trees, each trained on a subset of the input data (Breiman, 2001). Constructing these trees involves utilizing a random subset of features, a measure that mitigates the risk of model overfitting (Breiman, 2001). The final prediction materializes through aggregating the predictions of individual trees, accomplished through a process known as bagging or bootstrap aggregating. This averaging process serves to diminish model variance, rendering it more robust against noise and outliers in the data (Breiman, 2001). Random forest boasts several advantages over other machine learning algorithms, demonstrating robustness against overfitting—a prevalent issue in alternative algorithms. Furthermore, its capacity to handle high-dimensional data with numerous features and rank features based on their importance in the prediction process enhances its suitability for tackling complex problems.

In prospectivity modeling, the algorithm utilizes input data to identify a set of features relevant to the mineralization process. These features, in turn, train the random forest model, enabling the prediction of mineralization in a specified area. A notable advantage of employing random forest in prospectivity modeling is its proficiency in handling missing or noisy data, prevalent issues in geological data sets (Carranza & Laborte, 2015). Additionally, the algorithm accommodates both positive and negative training samples, contributing to the creation of a balanced data set. The application of this method extends to predicting the likelihood of various mineralization types and commodities (e.g., Carranza & Laborte, 2015; Farahbakhsh et al., 2023; Rodriguez-Galiano et al., 2014, 2015). Given that prospectivity modeling often involves extensive data sets with numerous features, random forest excels in handling such data without necessitating dimensionality reduction techniques. This is particularly crucial as certain features may play a pivotal role in predicting mineralization likelihood, and their removal could compromise the accuracy of the model.

In this study, the positive samples—representing mineral occurrences—range from minor prospects to giant deposits. Recognizing that these samples vary significantly in their economic importance, we employ cost-sensitive learning in our random forest classifier to account for this variability (Burez & Van den Poel, 2009). Cost-sensitive learning allows us to assign different weights to each training sample based on criteria reflecting their significance. Specifically, we assign weights from one to three to the training samples, proportional to their total metal content. Higher weights are given to samples with greater metal content, indicating larger and more economically valuable deposits. These weights are integrated into the training process such that samples with

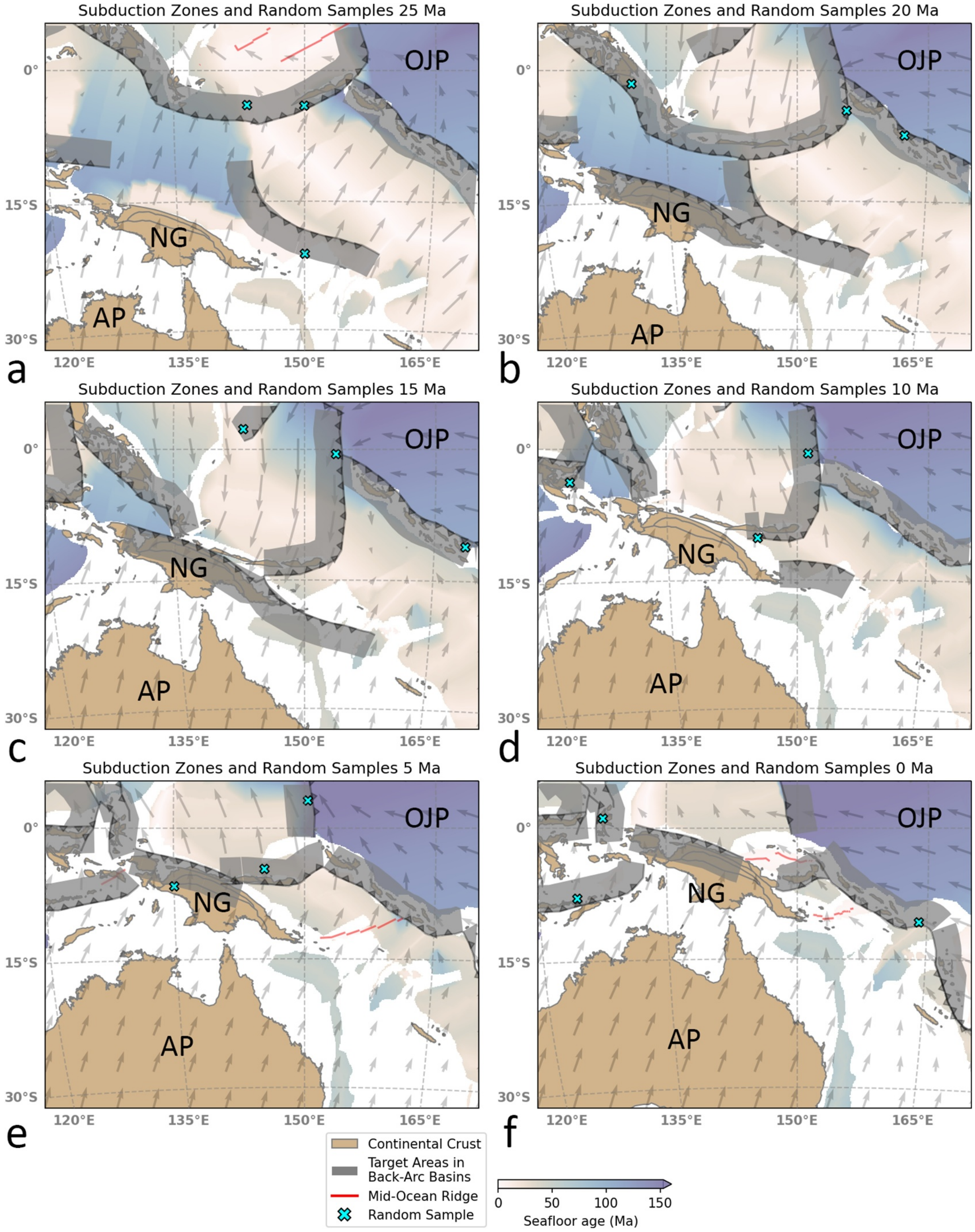

Figure 5. Buffer zones around the subduction zones covering back-arc basins, which are the target areas for creating prospectivity maps. As shown in the frames for 25 Ma to the present day (a–f), random or unlabeled samples are uniformly distributed through time and in these buffer zones. AP, Australian Plate; NG, New Guinea; OJP, Ontong Java Plateau.

higher weights have a greater probability of being included during the bootstrap sampling for each tree in the random forest. This approach biases the model to focus more on these significant samples. Additionally, the weights influence the calculation of node impurities during the tree-building process, further emphasizing the importance of correctly classifying higher-weighted samples (Burez & Van den Poel, 2009). By implementing this weighted approach, we aim to enhance the classifier's ability to predict significant mineral deposits, ensuring that it places appropriate emphasis on the most economically valuable occurrences. This method improves the model's performance by aligning it more closely with the practical priorities of mineral exploration.

4.4. Implementation

In this study, we leverage a range of Python libraries, for example, scikit-learn (Pedregosa et al., 2011), pyGPlates (R. D. Müller et al., 2018), and GPlately (Mather et al., 2024) to execute diverse tasks. These tasks encompass feature extraction, data cleaning, identification of missing values and outliers, visualization, comparison of various machine learning classifiers, selection of the most robust and successful classifier for the framework, hyperparameter tuning, and assessment of feature importance. Employing the co-registered data matrix, we construct a machine learning classifier, enabling predictions for exploration targets within one-sided buffer zones with a 3-degree width around trench lines covering back-arc basins in the study area (Figure 5) and also the entire New Guinea island.

Hyperparameter tuning involves selecting the optimal combination of hyperparameters for a machine learning model. Hyperparameters, distinct from model parameters learned during training, cannot be acquired through the learning process. The performance of a machine learning model is heavily reliant on the chosen hyperparameters, and finding the right combination can enhance accuracy, speed, and generalization ability. Thus, hyperparameter tuning is a pivotal aspect of constructing a robust and effective machine learning model. Various techniques, including grid search, random search, and Bayesian optimization (Alibrahim & Ludwig, 2021) are employed for this purpose. In this study, Bayesian optimization is utilized, employing a predictive model known as a surrogate to efficiently model the search space and identify optimal parameter combinations swiftly (Alibrahim & Ludwig, 2021). This tuning process holds particular significance when developing intricate models, characterized by numerous hyperparameters.

Highly correlated features are excluded from the modeling process based on the Spearman coefficient (Myers & Sirois, 2004). The prospectivity models, constructed using the plate motion models of R. D. Müller et al. (2016, 2019), are trained with 13 and 14 features, respectively, following the definition of significant correlation with a coefficient greater than 0.7 (Farahbakhsh et al., 2023). The Results section and Supporting Information S1 provide details on the correlations between various features and the selected input features. The selected features, combined with a set of known mineral occurrences as positive samples and a set of random samples, form the input for the PUB algorithm. After labeling the random samples as either positive or negative—where most are labeled negative due to the rarity of mineralization—these labeled samples, along with the actual positive samples, are used as input for the random forest classifier.

To optimize the performance of the random forest classifier, various hyperparameters must be carefully set. The crucial hyperparameter—the number of decision trees in the random forest—is set to 200 for both models. While increasing the number of trees can enhance accuracy, it may also escalate computational demands. Another vital hyperparameter is the maximum number of features for splitting a node, which is set to the square root of the total features for both models. A lower value promotes diversity among decision trees but may lead to overfitting. The maximum depth of each tree is fixed at 20 to balance accuracy improvement and the risk of overfitting. The minimum number of samples required to split an internal node is set to 2 for both models. A higher value encourages simpler decision trees, reducing overfitting but potentially compromising performance. Similarly, the minimum number of samples required at a leaf node is set to 2 for both models, influencing model generalizability and overfitting. Tuning these hyperparameters can significantly enhance the random forest classifier's performance in prospectivity modeling. Additionally, the number of unlabeled samples used to train each base estimator in the PUB classifier is tuned, with values set to 52 and 56 for the predictive models created based on the R. D. Müller et al. (2016, 2019) plate motion models. Careful tuning is essential to strike a balance and avoid underfitting or overfitting the model.

Using the fine-tuned classifier, we generate probability maps over regularly spaced grids with a resolution of 0.2°, covering the back-arc basins in the study area (Figure 5) and spanning from 30 Ma to the present day. Additionally, we predict mineralization probabilities for nodes spaced at 0.2-degree intervals across the entire New Guinea island at each time step from 30 Ma to the present. These probability values for each individual node are then used to calculate an overall probability. The map resolution is carefully chosen, taking into account the size of significant porphyry systems (Sillitoe, 2010) and considering the resolution of the input features. To assess model accuracy, we randomly conceal 20% of real positive samples from the machine learning model before creating a PUB model. The remaining positive samples, along with unlabeled samples, are utilized for model training. Additionally, we use a 10-fold cross-validation to evaluate the efficiency of our model in predicting

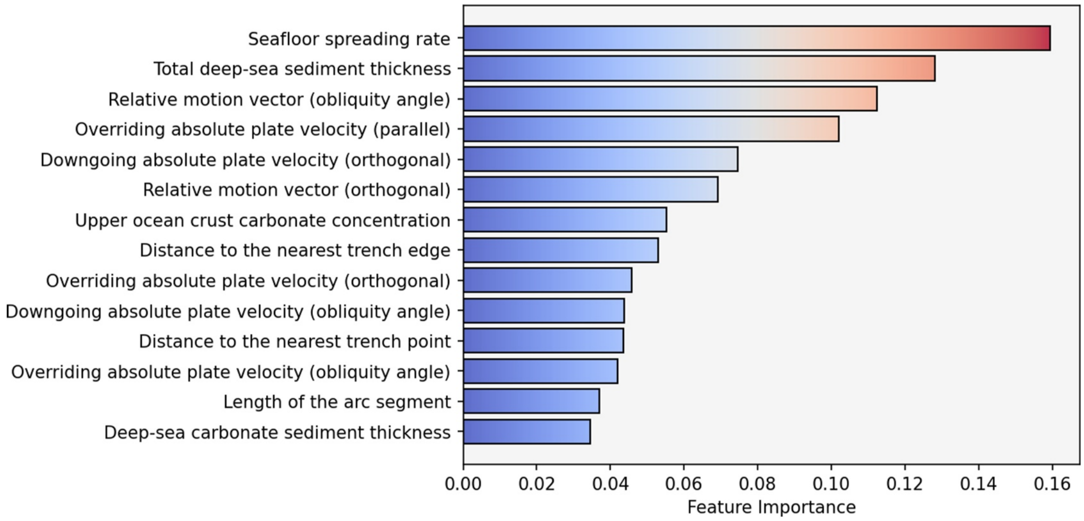

Figure 6. The importance of each feature in the formation and predicting porphyry systems in the New Guinea and Solomon Islands region determined by the random forest classifier based on the R. D. Müller et al. (2019) plate motion model.

different testing sets and avoid over-fitting. Given the limited number of geographically referenced positive labels, spatial autocorrelation effects are deemed negligible, and a random train/test split is considered optimal.

5. Results

The characteristics of deposits alone do not inherently establish causal relationships between specific features and the formation of porphyry systems. They must be considered in conjunction with a representation of the average feature functionality. For example, if barren areas exhibit a similar relationship to a specific feature compared to mineralized areas, it suggests that the feature is an identifying characteristic of barren areas. Conversely, when tectonic features associated with mineral occurrences deviate from the typical tectonics of the study area, it indicates a potential relationship to metallogenesis. Advanced data analyses through machine learning methods empower us to determine which tectonic features drive metallogenesis. The random forest method identifies robust connections in the data, discerning which feature interactions are likely key to porphyry genesis. This method learns which features are linked to mineralized areas and which are linked to barren areas. Random forest trains an ensemble of decision trees on a random subset of features and training examples with replacement. For prediction, the majority vote of the predictions by decision trees on a query point determines the class of the query point. This randomization process, often called bootstrap aggregating or bagging, is applied to both data points and features. As random forest employs bagging, it becomes straightforward to determine which features are essential for prediction. Given the considerations mentioned earlier, we primarily focus on the results obtained by employing the R. D. Müller et al. (2019) plate motion model and briefly compare them to the R. D. Müller et al. (2016) plate motion model in Supporting Information S1. The importance of each feature, determined by the random forest classifier based on the R. D. Müller et al. (2019) plate motion model for predicting potential mineralization zones, is presented in Figure 6. Random forest probabilities are determined as an out-of-bag accuracy (Breiman, 2001), providing a quantitative measure of feature importance by evaluating which decision trees contribute to the highest out-of-bag accuracy (Breiman, 2001). We observe fairly balanced importance of each feature in each scenario, as depicted in Figure 6, although these results may vary depending on the choice of training and testing sets.

According to Figure 6, the R. D. Müller et al. (2019) plate motion model designates seafloor spreading half-rate when the crust was formed, total deep-sea sediment thickness, the obliquity angle of the relative motion vector, and the parallel component of the overriding absolute plate velocity as the most important features. Other notable features include the orthogonal component of the downgoing absolute plate velocity and the orthogonal component of the relative motion vector. As previously mentioned, highly correlated features are removed from the training process to reduce the dimensionality of the feature space. It is also important to examine which features are correlated with those deemed highly significant. Figure 7 shows the hierarchical clustering

10.1029/2024TC008362

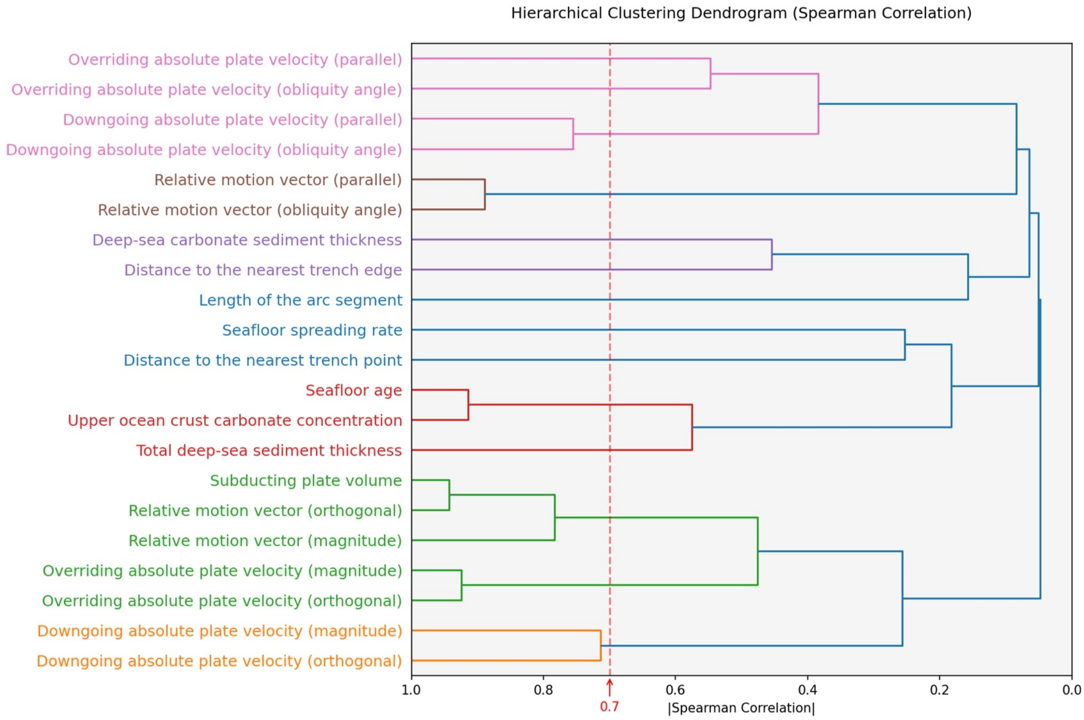

Figure 7. Hierarchical clustering dendrogram created for all the input features to the workflow, using the absolute value of Spearman correlation between them. Features displayed in the same color are considered correlated to varying degrees, with shorter branches indicating stronger correlations. As shown, the vertical dashed line indicating the defined threshold of 0.7 cuts the branches at 14 points, corresponding to the number of features used to train the model.

dendrogram based on the absolute value of the Spearman correlation coefficient, revealing patterns in the relationships among various tectonic and seafloor characteristics. Features related to absolute plate velocity for both overriding and downgoing plates cluster together, suggesting strong similarities in their behavior across different measurements, including parallel and orthogonal components, obliquity angle, and magnitude. Similarly, sediment and crustal properties, including total deep-sea sediment thickness, upper ocean crust carbonate concentration, and seafloor age, form a distinct cluster, indicating a correlation among sedimentary and crustal features of oceanic plates.

Figure 8 displays violin-box plots comparing positive and negative samples, highlighting differences in the range and distribution of values for the most influential features identified in the formation of porphyry systems in the study area, based on the R. D. Müller et al. (2019) plate motion model. Across all the features, negative samples generally show a wider range and more dispersed values, while positive samples are more tightly clustered with narrower ranges and generally higher medians in most plots. In Figure 8a, representing the seafloor spreading half-rate, negative samples exhibit a broader range from around 10 to 80 mm/yr with a concentration around 20 to 40, while positive samples are more consistent, centered around 30–45 mm/yr. This pattern of higher variability in negative samples continues in the plot for total deep-sea sediment thickness (Figure 8b), where negative samples range from approximately 50 to 850 m, primarily in the lower half, compared to the positive samples, which are more uniformly distributed between 100 and 200 m. Similarly, for the obliquity angle of the relative motion vector, negative samples have a broad range from around −55 to 80°, while positive samples are concentrated between 0 and 85°, indicating tighter grouping in positive samples (Figure 8c). In terms of the parallel component of the overriding absolute plate velocity, negative samples span from −15 to 12 cm/yr, whereas positive samples are more consistent, ranging narrowly between −14 and 2 cm/yr (Figure 8d). As shown in Figure 8e, this trend of higher spread in negative samples also appears in the orthogonal component of the downgoing absolute plate velocity, where negative values range from around −9 to 9 cm/yr, and positive samples are closely clustered between −5 and 12 cm/yr. Lastly, for the orthogonal component of the relative motion vector, negative samples display a wider range from −6 to 15 cm/yr, while positive samples are concentrated around −6 to 13 cm/yr with a higher median (Figure 8f).

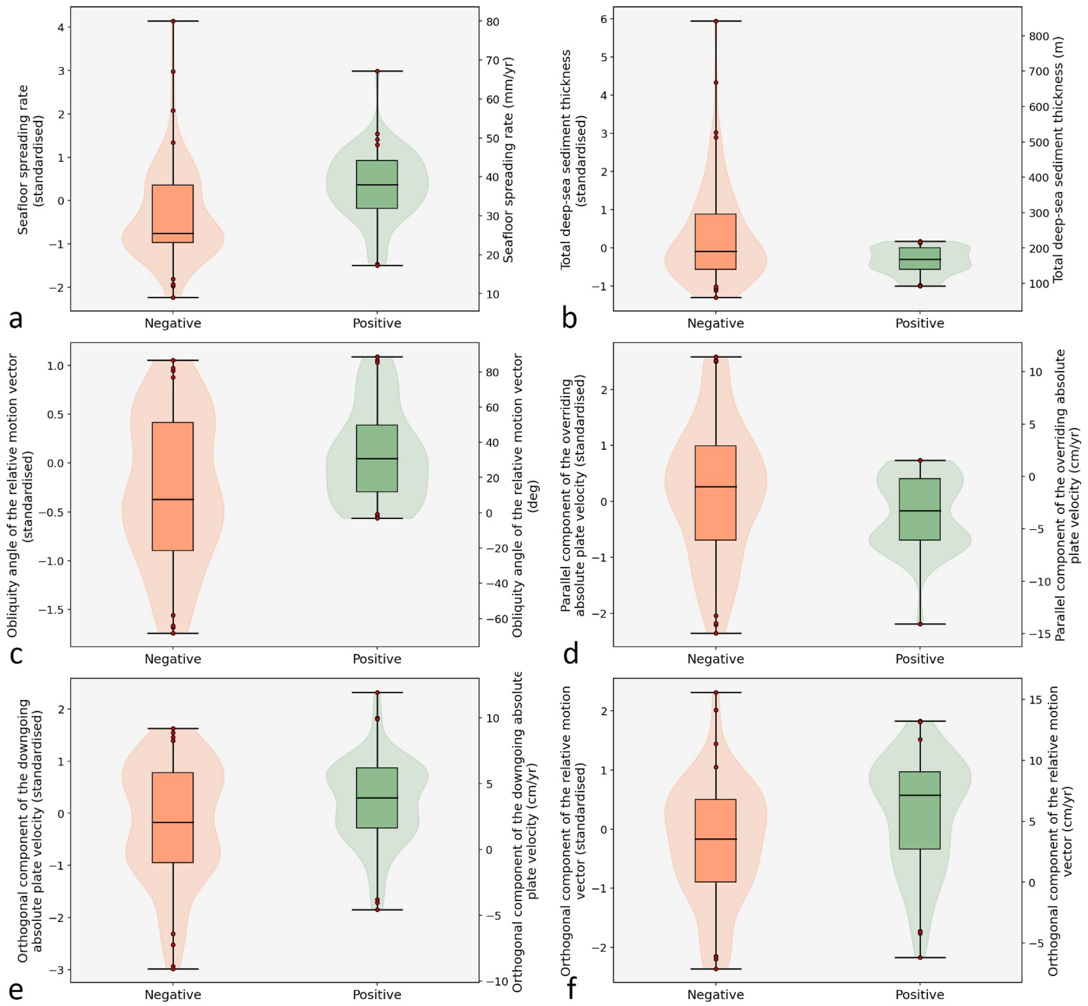

Figure 8. Violin-box plots of the positive and negative samples for the most important features determined based on the R. D. Müller et al. (2019) plate motion model (Figure 6) including (a) seafloor spreading half-rate, (b) total deep-sea sediment thickness, (c) the obliquity angle of the relative motion vector, (d) the parallel component of the overriding absolute plate velocity (e) the orthogonal component of the downgoing absolute plate velocity, and (f) the orthogonal component of the relative motion vector.

Selected independent features capture the evolving dynamics of subduction zones during the formation of porphyry systems, exhibiting distinct characteristics from barren areas. These features can serve as the foundation for constructing a predictive model to discern mineralized regions. The model's performance can be evaluated using various metrics. In the absence of a set of real negative samples, the evaluation relies on using the real positive samples to measure accuracy. The predictive model based on the R. D. Müller et al. (2019) plate motion model successfully predicts 89.65% of mineral occurrences in the testing data set. However, this performance may be influenced by data bias, potentially stemming from the extensive study area and the uneven distribution of negative samples across both time and space. The spatio-temporal model generates a series of prospectivity maps, delineating the likelihood of porphyry mineralization throughout the subduction history within the study area. Figure 9 presents six frames of the predictive model based on the R. D. Müller et al. (2019) plate motion model, covering back-arc basins. Additionally, Figure 10 shows the porphyry mineralization probability for a set of nodes within the current extent of New Guinea, reconstructed back to 30 Ma. Each target point is assigned a score ranging from 0 to 1, denoting the probability of the point being barren (zero) or fertile (one). These scores provide a nuanced understanding of the potential mineralization across the study area, offering valuable insights for further exploration and resource management.

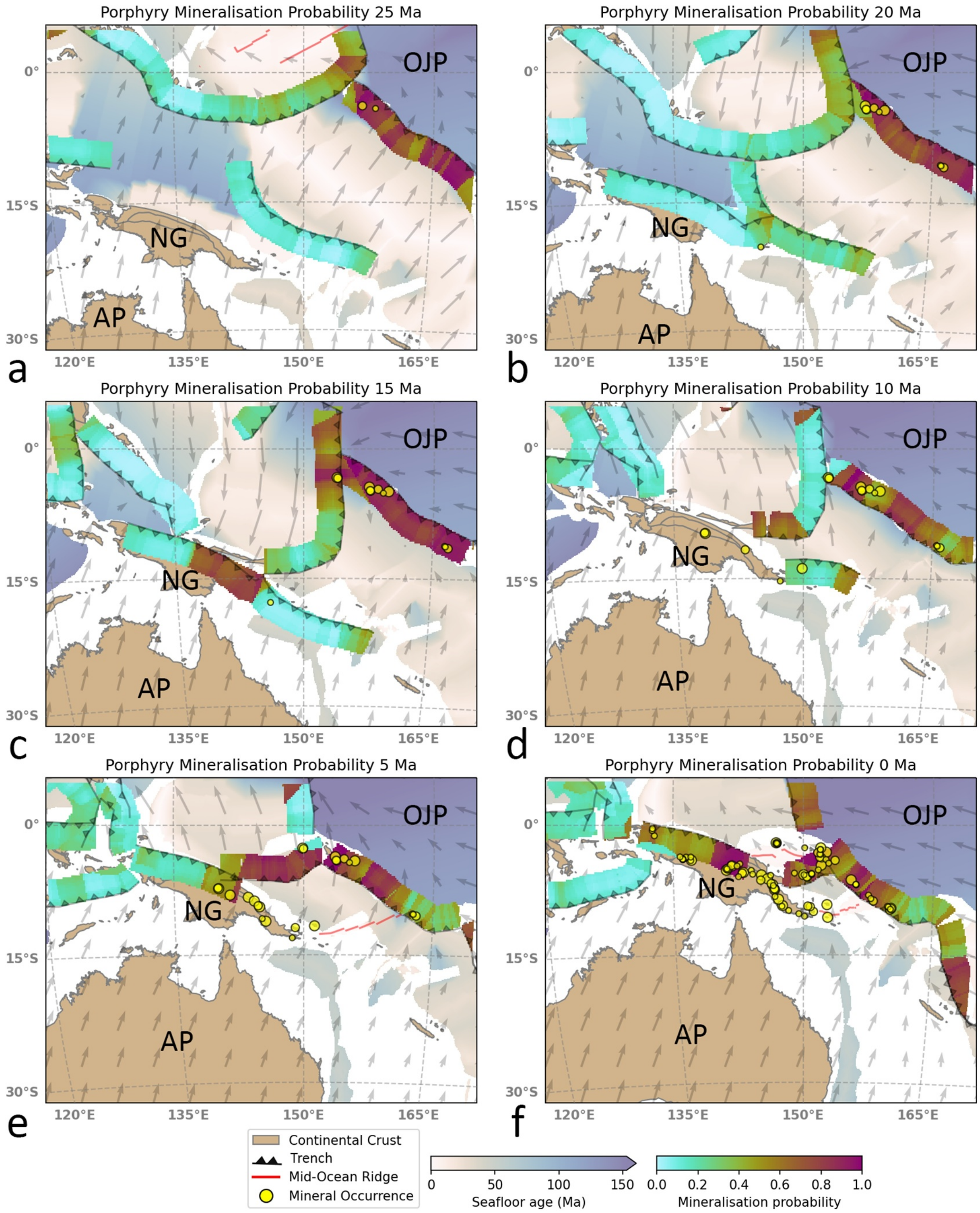

Figure 9. Spatio-temporal prospectivity maps of porphyry mineralization in the back-arc basins surrounding the New Guinea and Solomon Islands region, including known porphyry mineral occurrences, generated using the R. D. Müller et al. (2019) plate motion model from 30 Ma to the present day (a–f). Probability values range from 0 to 1, indicating the likelihood of the target area being barren (zero) or fertile (one). AP, Australian Plate; NG, New Guinea; OJP, Ontong Java Plateau.

To create a prospectivity map for porphyry mineralization across the entire New Guinea island and to summarize the spatio-temporal model in a single representation, we assign to each node within the current extent of New Guinea the median probability (where values exceed 0.5) calculated from 30 Ma to the present. We then interpolate these probability values to produce the map shown in Figure 11a. To further evaluate our approach, we generate a prediction-area plot, shown in Figure 11b, which illustrates the relationship between the predicted mineral potential area and the actual occurrences of mineral deposits. This plot provides insight into the effectiveness of our predictive model in identifying areas with high mineral potential. Unlike common metrics like

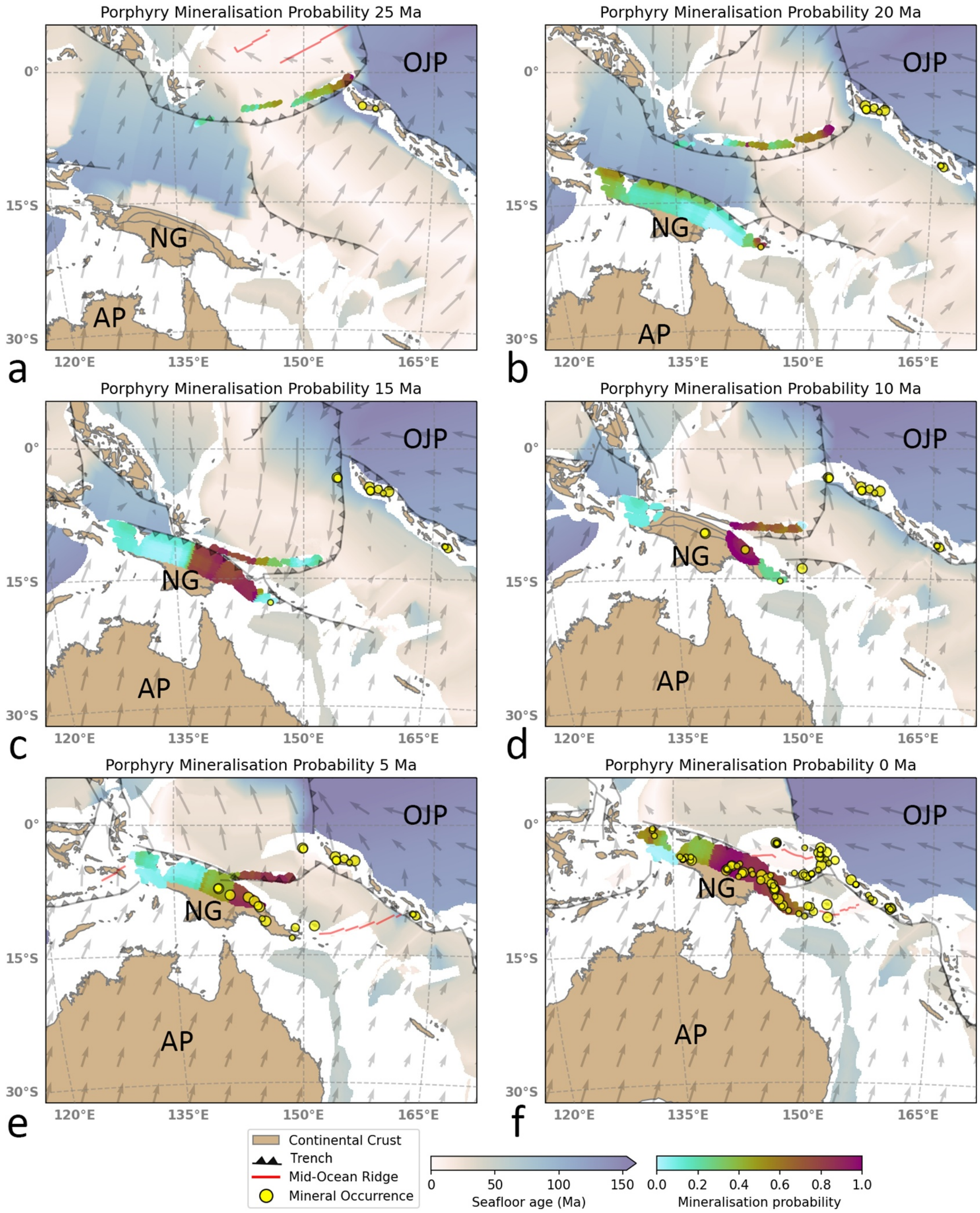

Figure 10. Porphyry mineralization probability at the nodes located within the current extent of the New Guinea island generated using the R. D. Müller et al. (2019) plate motion model from 30 Ma to the present day (a–f). Probability values range from 0 to 1, indicating the likelihood of the target point being barren (zero) or fertile (one). AP, Australian Plate; NG, New Guinea; OJP, Ontong Java Plateau.

accuracy, prediction-area plots are particularly useful in geological studies as they incorporate the spatial distribution of predictions, which is critical for resource exploration. Additionally, these plots indicate the proportion of the area that must be explored to locate a given percentage of deposits, aiding in efficient resource allocation. In Figure 11b, we observe that with a probability threshold of 0.79, 60% of known mineral occurrences are captured within 40% of the study area. This is a promising result, given that the model relies solely on features derived from a plate motion model. Further improvements could be achieved by reducing the spacing between the nodes within the study area and the trench points along trench lines from which features are extracted.

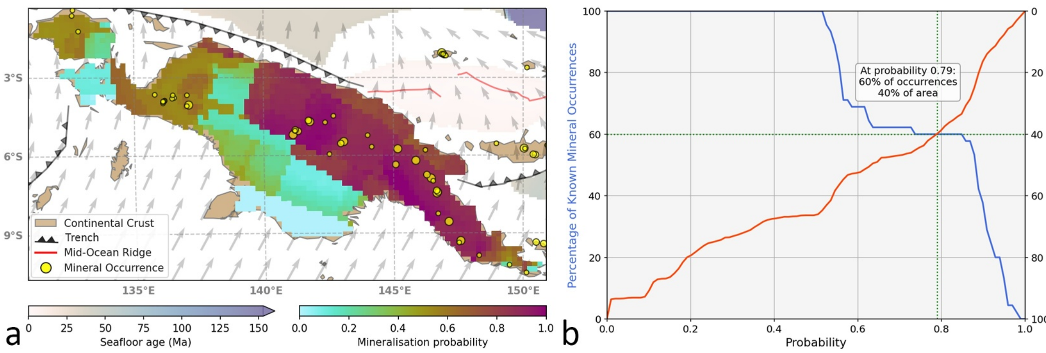

Figure 11. (a) Porphyry mineralization prospectivity map of New Guinea created using a set of spatio-temporal features obtained by R. D. Müller et al. (2019) plate motion model representing tectonic and seafloor characteristics of the subduction zones from 30 Ma to present day. (b) Prediction-area plot for the prospectivity model illustrating the relationship between the predicted mineral potential area and the actual occurrence of mineral deposits.

6. Discussion

Creating spatio-temporal mineral prospectivity models allows exploration geologists to unravel the intricate temporal evolution of tectonic features, facilitating more precise predictions of favorable mineralization conditions through time. These models can help to optimize greenfield exploration efforts by de-risking areas with a higher likelihood of hosting porphyry deposits, ultimately enhancing the efficiency and success rates of mineral exploration campaigns. Based on the model developed in this study, key predictors for porphyry mineralization in the New Guinea and Solomon Islands region, using the R. D. Müller et al. (2019) plate motion model, include seafloor spreading half-rate, total deep-sea sediment thickness, and the obliquity angle of the relative motion vector. Other notable features include three velocity vectors: the parallel component of the overriding absolute plate velocity, the orthogonal component of the downgoing absolute plate velocity, and the orthogonal component of the relative motion vector. While no single feature independently serves as a statistically robust predictor for porphyry system formation, the simultaneous consideration of multiple features under specific conditions increases the likelihood of porphyry magmatism. Traditional studies that concentrate on single parameters might account for the variations in comprehending the underlying formation mechanisms linked to tectonic processes. These discrepancies arise because such studies often overlook the complexity and interconnectivity of factors influencing tectonic phenomena. By focusing narrowly on individual aspects, without considering the holistic view of geological processes, researchers may miss critical insights into how various elements interact to drive the dynamics of the Earth's crust. This limitation underscores the importance of adopting more integrative approaches that consider multiple parameters simultaneously to gain a deeper, more accurate understanding of tectonic mechanisms (Bertrand et al., 2014; Sillitoe, 2010; Tosdal & Richards, 2001). The absence of a single dominant feature in class determination (e.g., Figure 6) suggests that individual features alone are insufficient for successful porphyry system formation, aligning with J. P. Richards (2003), who posits that these systems result from the integration and optimization of multiple tectono-magmatic processes.

The most crucial feature identified for creating the prospectivity model using the (R. D. Müller et al., 2019) plate motion model is the seafloor spreading half-rate of the subducting crust, related to when the subducting crust originally formed. It emerges as a key feature with distinct associations in mineralized areas, showcasing a specific range of values, especially from 30 to 45 mm/yr. This feature exhibits no pronounced correlation with other features, yet it demonstrates the highest positive correlation with the obliquity angle of the relative motion vector and the most substantial negative correlation with total deep-sea sediment thickness. The interplay of seafloor spreading rate and seafloor roughness, indicative of faulting, is evident, with lower spreading rates contributing to higher roughness (Malinverno, 1991; Whittaker et al., 2008), providing conducive pathways for magmatic ascent near the surface. Lower to moderate spreading rates result in a higher proportion of serpentinized mantle peridotite, introducing additional water and carbon to the plate as compared to higher spreading rates (Merdith et al., 2020). During subduction, these components are expelled, fostering increased hydrous melting in the mantle wedge and serving as a catalyst for porphyry mineralization (Merdith et al., 2020). This aligns with the recent study by Alfonso et al. (2024), which suggests that an adequate supply of volatile fluids into the subduction system is a key prerequisite for mineralization. The study also identifies seafloor spreading rate as an important factor in modeling porphyry mineralization prospectivity.

The total deep-sea sediment thickness is also a key feature for distinguishing between mineralized and barren areas. In our prospectivity model, positive samples exhibit a specific range of values (100–200 m) compared to negative samples, suggesting a correlation between mineralization and this sediment thickness range. It has been proposed that metals found in porphyry systems may have origins in divergent margins, where seafloor generated at spreading ridges can host volcanic-associated massive sulfide deposits with variable copper content due to enrichment from hydrothermal activity or source magma composition (Hattori & Keith, 2001; Meinert, 2007; Qu et al., 2004; Sillitoe, 1972). As the oceanic lithosphere ages and thickens, it often accumulates sediment and experiences chemical transformations that increase its potential for contributing metals to subduction-related magmatism. The accumulation of sediments on older seafloor can contribute to increased melt volume during subduction, although the influence of these factors is still debated (Qu et al., 2004). Our results show only a weak correlation between sediment thickness and mineralization, suggesting that a combination of factors, rather than sediment or metal content alone, may enhance porphyry formation. Total deep-sea sediment thickness may serve as a proxy for water content subducted with the slab, which is subsequently released as fluids that metasomatize the overlying asthenospheric mantle wedge, thereby promoting the formation of porphyry systems in the overriding plate (J. P. Richards, 2003, 2014).

The obliquity angle of the relative motion vector, as illustrated in Figure 6, is the third most important feature. This feature, especially within the 15 to 45-degree range (Figure 8), shows a positive correlation with porphyry mineralization in the study area, highlighting the critical role of subduction obliquity in the formation of porphyry systems (Figure 6). This is in contrast with Butterworth et al. (2016), who suggested that porphyry systems in South America tend to form preferentially when subduction obliquity is nearly trench-perpendicular. However, the South American subduction system is much longer in its spatial extent and more long-lived than our study area. The observed difference suggests that not all subduction systems favor the same combination of parameters for porphyry ore deposit generation. In our study, the results indicate that oblique convergence in subduction zones is more likely to lead to mineralization in the New Guinea and Solomon Islands region. The influence of obliquity angle extends to fluid flow, magmatic processes, and stress regimes in the subduction zone (Plunder et al., 2018), impacting the transport of mineralizing elements and creating favorable conditions for ore deposition.

Three velocity vectors emerge among the important features. As shown in Figure 6, elevated values in the orthogonal components of the downgoing absolute plate velocity and the relative motion vector, along with lower values in the parallel component of the overriding absolute plate velocity, are aligned with mineralization. The higher orthogonal velocity of the downgoing plate is implicated in increasing the subducting plate volume, expediting metasomatism and partial melting processes. These processes play a crucial role in initiating the formation of porphyry systems within the overriding plate (Bertrand et al., 2014) and have been highlighted in previous studies, particularly in the Americas (Alfonso et al., 2024; Butterworth et al., 2016; Diaz-Rodriguez et al., 2021).

The prospectivity model developed based on the R. D. Müller et al. (2019) plate motion model indicates that oblique subduction zones are more likely to host porphyry systems. This likelihood is heightened when combined with a high orthogonal absolute velocity of the downgoing plate and a low to moderate seafloor spreading half-rate, leading to increased melt and facilitating the percolation of porphyry melts to the near-surface. A comprehensive understanding of these features over time empowers exploration geologists to evaluate potential locations for porphyry systems, particularly in the evolving geological history of the New Guinea and Solomon Islands region. The predicted probabilities of porphyry magmatism in the time-space maps essentially represent the reconstructed positions where present-day mineral occurrences are likely to have formed.

Spatio-temporal prospectivity models allow us to trace the locations of known mineral occurrences over time. We compare the variations of key features in the development of porphyry systems based on the R. D. Müller et al. (2019) model against the changes in the probability of mineralization for the well-documented Panguna deposit (Figure 12). The analysis suggests that mineralization in this deposit is driven by factors like seafloor spreading rates, sediment thickness, and specific aspects of plate motion. Higher seafloor spreading rates and oblique subductions appear to create optimal conditions for mineralization. Similarly, thicker sediment layers and the orthogonal movement of the downgoing plate are positively associated with increased mineralization

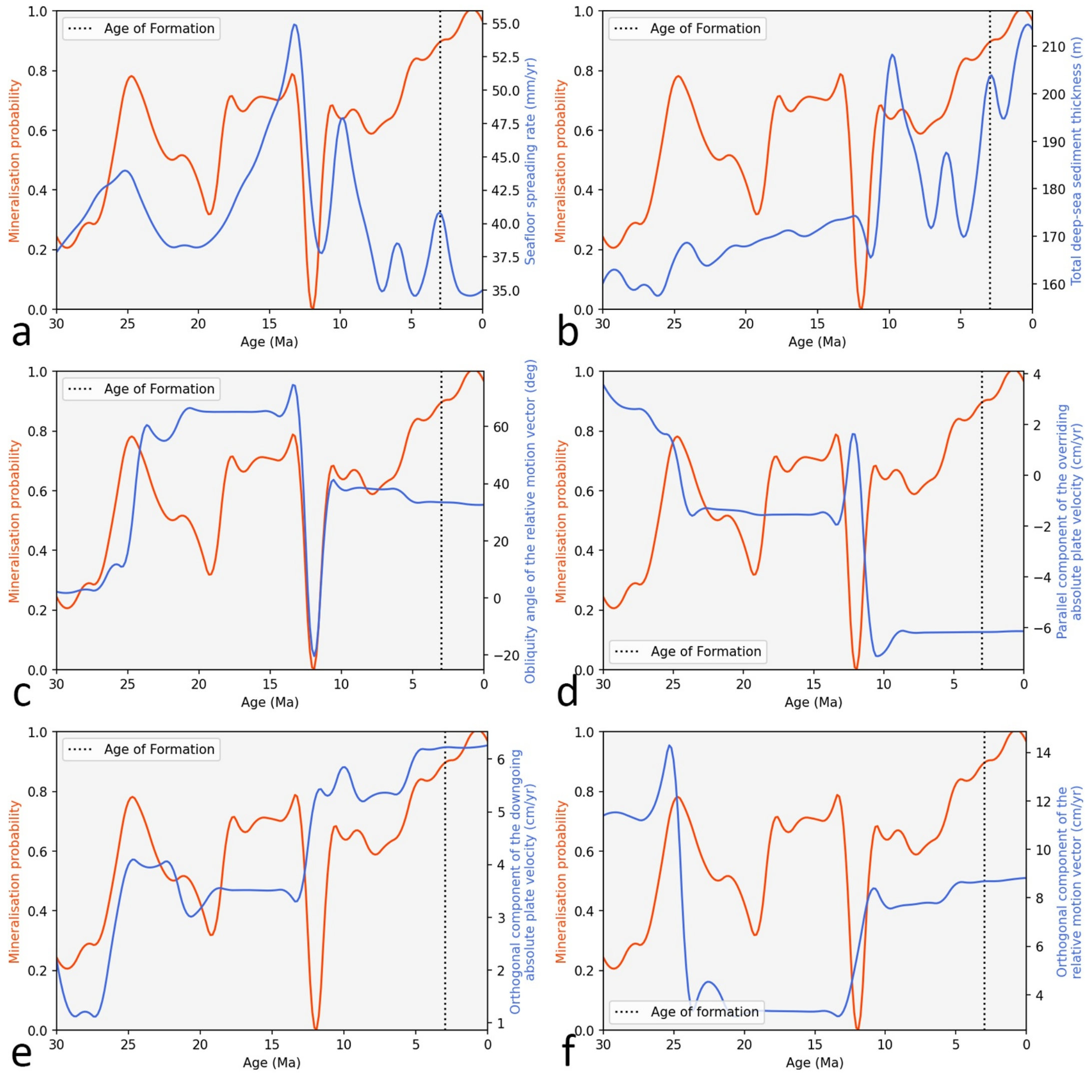

Figure 12. Variations of mineralization probability and important feature values including (a) seafloor spreading half-rate, (b) total deep-sea sediment thickness, (c) the obliquity angle of the relative motion vector, (d) the parallel component of the overriding absolute plate velocity (e) the orthogonal component of the downgoing absolute plate velocity, and (f) the orthogonal component of the relative motion vector determined based on the R. D. Müller et al. (2019) plate motion model at the reconstructed locations of Panguna porphyry Cu-Au deposit since 30 Ma.

probability, indicating that these factors favor mineralization processes. This interplay suggests that periods of ideal spreading rates, substantial sediment coverage, and enhanced downgoing plate movement likely boost mineralization events, while disruptions from particular plate motions or sedimentation processes may reduce the likelihood of mineralization.

In their review papers on the tectonic setting of porphyry copper mineralization, Sillitoe (1997) and Cooke et al. (2005) emphasize the importance of collisional tectonics in impeding magma ascent, leading to the formation of large, shallow magma chambers characterized by magmatic-hydrothermal fluids. This contrasts with extensional arc settings, as collisional environments create conditions that promote rapid uplift and erosion, placing these magma chambers near the surface and making them accessible for mining. These points are well illustrated by Holm et al. (2019), who identify two key tectonic events that have influenced Cu mineralization in the region: the Australia-Papua New Guinea collision around 11 Ma, associated with copper-rich deposits in the west and the Ontong Java-Solomon Islands hard collision from 5 to 0 Ma, associated with significant copper deposits in the east. These collisions effectively explain the formation of high-tonnage copper deposits observed in both western and eastern parts of the study area.

Building upon these insights, the characteristics and formation of mineral deposits in the study area also reveal a strong connection to local tectonic activities. The formation of copper-rich deposits in the Melanesian Arc in northern Papua New Guinea around 24 to 20 Ma, although a minor event in terms of total endowment, coincided with significant tectonic changes such as the collision of the Ontong Java Plateau (Holm et al., 2019). A notable shift occurred around 6 Ma with the emergence of copper-gold deposits in the West Bismarck, New Britain, and Solomon arcs. This period marked a significant phase of gold enrichment and tectonic activity, characterized by numerous gold-rich deposits and linked to the advent of microplate tectonics in the region. Remarkably, high probability values in Figure 12 highlight the presence of this recent metallogenic episode.

In the New Guinea Orogen, two distinct tectonic phases influenced mineral deposit formation. The initial phase, spanning approximately 12 to 6 Ma, was associated with the Australian continental collision and led to a significant accumulation of copper-rich minerals despite the relatively limited number of discovered deposits. This aligns with the findings of Sillitoe (1997) and Cooke et al. (2005), who noted that collisional tectonics played a crucial role in forming such deposits by impeding magma ascent and fostering large shallow magma chambers. The subsequent phase, beginning around 6 Ma and possibly linked to delamination of the Earth's crust, witnessed the formation of numerous known deposits (Figure 11a). This phase corresponds to the Ontong Java-Solomon Islands collision outlined by Holm et al. (2019), reflecting a period marked by continued tectonic activity and metallogenesis in response to evolving microplate interactions and continental collisions. These tectonic events not only shaped the distribution and characteristics of copper and gold deposits but also highlight the broader interplay between tectonic processes, magma evolution, and mineralization within the region.

The success of employing machine learning in mineral prospectivity modeling hinges on effectively characterizing the data set at hand, and the methods outlined in this study offer scalability as more data become available. The robustness of the results could be further enhanced with improvements in the spatio-temporal resolution of various parameters or features, such as plate models, age grids, temporal binning, and trench partitioning. The findings reveal that known porphyry systems align with areas of high prospectivity, with the R. D. Müller et al. (2019) plate motion model correctly predicting the majority of them. Despite uncertainties in global plate motion models, oceanic grids, and geochronologic methods, the overall high correlation between porphyry mineralization and proposed high prospectivity areas suggests that misclassification is more of an exception than a rule. These results carry significant implications for mineral exploration, emphasizing the importance of specific conditions in both the downgoing plate and the subduction trench for porphyry system formation. Integration with conventional data layers can facilitate the selection of prospective intrusive belts, even beneath the cover. The continuous refinement of the model—integrating new data on crustal thickness, enhanced tectonic models, and factors such as collisional and post-collisional events, stress regimes, and magma rheology, along with comprehensive geological, geochemical, and geophysical data from overriding plates—paves the way for multiple opportunities to improve the model. It is particularly worth noting that our workflow currently lacks consideration for the geology of the overriding plate, including structural fabric, nature of the basement, erosion, and weathering, which can be incorporated into future models. Our model offers valuable insights into the broader regional conditions influencing deposit formation, providing a framework for understanding the large-scale factors conducive to deposit occurrence. However, it is crucial to recognize that at a more localized level, exceptions to these conditions arise due to the dynamic nature of geological settings. In the southwest Pacific and Southeast Asia, instances of continental accretion occurred throughout the Cenozoic (Audley-Charles, 1981; Hill & Hall, 2003; Holm et al., 2013, 2015; Petterson et al., 1999), and small tectonic plates formed at increasingly smaller scales (Holm et al., 2016; Wallace et al., 2004). By integrating plate boundary-scale processes through time with the inherent anomalies at regional and district scales within Earth systems, we can enhance our insights into metallogenesis and improve the effectiveness of mineral exploration.

7. Conclusions

Our spatio-temporal mineral prospectivity models offer valuable insights for exploration geologists seeking to understand and predict porphyry system formation in the New Guinea and Solomon Islands region. Key predictors identified using the R. D. Müller et al. (2019) model include seafloor spreading half-rate, total deep-sea sediment thickness, and the obliquity angle of the relative motion vector, along with specific orthogonal and parallel components of the velocity vectors for both downgoing and overriding plates. Although no single feature serves as a strong predictor on its own, combining multiple features—particularly those related to subduction obliquity, convergence rate, and seafloor characteristics—significantly enhances the reliability of prospectivity models. The seafloor spreading rate, which formed the subducting crust, plays a significant role in creating conducive conditions for porphyry mineralization. Contrary to previous suggestions, highly oblique subduction zones are found to be more likely mineralization-rich in our study area, with large obliquity angles enhancing strain partitioning, fluid flow, and magmatic processes. The orthogonal component of the downgoing absolute plate velocity emerges as a crucial feature, impacting tectonic stresses and subducting plate volume. Our results and open-source workflow contribute to the nuanced understanding of the complex interplay of geological and tectonic factors influencing porphyry system formation, offering practical guidance for exploration efforts and refining predictive models to identify prospective areas for porphyry deposits in the studied region.

Data Availability Statement

The Jupyter notebook that this analysis is based on containing a Python workflow to calculate mineralization probability using a plate reconstruction model is archived online in Farahbakhsh et al. (2024) at https://doi.org/10.5281/zenodo.10976576. The GPlates software suit, for example, GPlates, pyGPlates, and GPlately used for reconstructing and plotting tectonic plate movements are freely available from https://gplates.org/download.

Acknowledgments

EF, SZ, BM, FK, MS, and RDM acknowledge funding from the Australian Research Council Grant LP210100173. SZ was supported by the Australian Research Council Grant DE210100084 and a University of Sydney Robinson Fellowship. MS acknowledges funding from the Australian Research Council Grant DP200100966. GPlates and pyGPlates development is funded by the AuScope National Collaborative Research Infrastructure System (NCRIS) program. Open access publishing facilitated by The University of Sydney, as part of the Wiley - The University of Sydney agreement via the Council of Australian University Librarians.

References

Abbott, L. D. (1995). Neogene tectonic reconstruction of the Adelbert-Finisterre-New Britain collision, northern Papua New Guinea. *Journal of Southeast Asian Earth Sciences*, *11*(1), 33–51. https://doi.org/10.1016/0743-9547(94)00032-A

Alfonso, C. P., Müller, R. D., Mather, B., & Anthony, M. (2024). Spatio-temporal copper prospectivity in the American Cordillera predicted by positive-unlabeled machine learning. *GSA Bulletin*, *137*(1–2), 702–711. https://doi.org/10.1130/B37614.1

Alibrahim, H., & Ludwig, S. A. (2021). Hyperparameter optimization: Comparing genetic algorithm against grid search and Bayesian optimization. In *IEEE Congress on Evolutionary Computation* (pp. 1551–1559). https://doi.org/10.1109/CEC45853.2021.9504761

Audley-Charles, M. G. (1981). Geometrical problems and implications of large scale over-thrusting in the Banda Arc-Australian margin collision zone. *Geological Society, London, Special Publications*, *9*(1), 407–416. https://doi.org/10.1144/GSL.SP.1981.009.01.37

Bertrand, G., Guillou-Frottier, L., & Loiselet, C. (2014). Distribution of porphyry copper deposits along the western Tethyan and Andean subduction zones: Insights from a paleotectonic approach. *Ore Geology Reviews*, *60*, 174–190. https://doi.org/10.1016/j.oregeorev.2013.12.015

Breiman, L. (2001). Random forests. *Machine Learning*, *45*(1), 5–32. https://doi.org/10.1023/A:1010933404324

Burez, J., & Van den Poel, D. (2009). Handling class imbalance in customer churn prediction. *Expert Systems with Applications*, *36*(3), 4626–4636. https://doi.org/10.1016/j.eswa.2008.05.027

Butterworth, N., Steinberg, D., Müller, R. D., Williams, S., Merdith, A. S., & Hardy, S. (2016). Tectonic environments of South American porphyry copper magmatism through time revealed by spatiotemporal data mining. *Tectonics*, *35*(12), 2847–2862. https://doi.org/10.1002/2016TC004289

Carranza, E. J. M., & Laborte, A. G. (2015). Random forest predictive modeling of mineral prospectivity with small number of prospects and data with missing values in Abra (Philippines). *Computers & Geosciences*, *74*, 60–70. https://doi.org/10.1016/j.cageo.2014.10.004

Carranza, E. J. M., & Laborte, A. G. (2016). Data-driven predictive modeling of mineral prospectivity using random forests: A case study in Catanduanes Island (Philippines). *Natural Resources Research*, *25*(1), 35–50. https://doi.org/10.1007/s11053-015-9268-x

Chiaradia, M., & Caricchi, L. (2022). Supergiant porphyry copper deposits are failed large eruptions. *Communications Earth & Environment*, *3*(1), 107. https://doi.org/10.1038/s43247-022-00440-7

Church, C., & Crawford, A. (2020). Minerals and the metals for the energy transition: Exploring the conflict implications for mineral-rich, fragile states. In M. Hafner & S. Tagliapietra (Eds.), *The geopolitics of the global energy transition* (pp. 279–304). Springer International Publishing. https://doi.org/10.1007/978-3-030-39066-2_12

Cooke, D. R., Agnew, P., Hollings, P., Baker, M., Chang, Z., Wilkinson, J. J., et al. (2020). Recent advances in the application of mineral chemistry to exploration for porphyry copper–gold–molybdenum deposits: Detecting the geochemical fingerprints and footprints of hypogene mineralization and alteration. *Geochemistry: Exploration, Environment, Analysis*, *20*(2), 176–188. https://doi.org/10.1144/geochem2019-039

Cooke, D. R., Hollings, P., & Walshe, J. L. (2005). Giant porphyry deposits: Characteristics, distribution, and tectonic controls. *Economic Geology*, *100*(5), 801–818. https://doi.org/10.2113/gsecongeo.100.5.801

Craig, M., & Warvakai, K. (2009). Structure of an active foreland fold and thrust belt, Papua New Guinea. *Australian Journal of Earth Sciences*, *56*(5), 719–738. https://doi.org/10.1080/08120090903005360

Crowhurst, P. V., Maas, R., Hill, K. C., Foster, D. A., & Fanning, C. M. (2004). Isotopic constraints on crustal architecture and Permo-Triassic tectonics in New Guinea: Possible links with eastern Australia. *Australian Journal of Earth Sciences*, *51*(1), 107–124. https://doi.org/10.1046/j.1400-0952.2003.01046.x

Davies, H. L. (2012). The geology of New Guinea-the cordilleran margin of the Australian continent. *Episodes Journal of International Geoscience*, *35*(1), 87–102. https://doi.org/10.18814/epiiugs/2012/v35i1/008

Diaz-Rodriguez, J., Müller, R. D., & Chandra, R. (2021). Predicting the emplacement of Cordilleran porphyry copper systems using a spatio-temporal machine learning model. *Ore Geology Reviews*, *137*, 104300. https://doi.org/10.1016/j.oregeorev.2021.104300

Dutkiewicz, A., Müller, R. D., Cannon, J., Vaughan, S., & Zahirovic, S. (2018). Sequestration and subduction of deep-sea carbonate in the global ocean since the Early Cretaceous. *Geology*, *47*(1), 91–94. https://doi.org/10.1130/G45424.1

Dutkiewicz, A., Müller, R. D., Wang, X., O'Callaghan, S., Cannon, J., & Wright, N. M. (2017). Predicting sediment thickness on vanished ocean crust since 200 Ma. *Geochemistry, Geophysics, Geosystems*, *18*(12), 4586–4603. https://doi.org/10.1002/2017GC007258

Farahbakhsh, E., Maughan, J., & Müller, R. D. (2023). Prospectivity modelling of critical mineral deposits using a generative adversarial network with oversampling and positive-unlabelled bagging. *Ore Geology Reviews*, *162*, 105665. https://doi.org/10.1016/j.oregeorev.2023.105665

Farahbakhsh, E., Zahirovic, S., McInnes, B. I. A., Polanco, S., Kohlmann, F., Seton, M., & Müller, R. D. (2024). Machine learning-based spatiotemporal prospectivity modeling of porphyry systems in the New Guinea and Solomon Islands region [Software]. *Zenodo*. https://doi.org/10.5281/zenodo.10976576

Figueroa, R. L., Zeng-Treitler, Q., Kandula, S., & Ngo, L. H. (2012). Predicting sample size required for classification performance. *BMC Medical Informatics and Decision Making*, *12*(1), 1–10. https://doi.org/10.1186/1472-6947-12-8
Gan, S., Alshahrani, M., & Liu, S. (2022). Positive-unlabeled learning for network link prediction. *Mathematics*, *10*(18), 3345. https://doi.org/10.3390/math10183345
Hall, R. (2002). Cenozoic geological and plate tectonic evolution of SE Asia and the SW Pacific: Computer-based reconstructions, model and animations. *Journal of Asian Earth Sciences*, *20*(4), 353–431. https://doi.org/10.1016/S1367-9120(01)00069-4
Hammarstrom, J. M., Bookstrom, A. A., Dicken, C. L., Drenth, B. J., Ludington, S., Robinson, G. R., Jr., et al. (2013). *Porphyry copper assessment of Southeast Asia and Melanesia: Chapter D in Global mineral resource assessment* (Technical Report). U.S. Geological Survey. https://doi.org/10.3133/sir20105090D
Hattori, K. H., & Keith, J. D. (2001). Contribution of mafic melt to porphyry copper mineralization: Evidence from Mount Pinatubo, Philippines, and Bingham Canyon, Utah, USA. *Mineralium Deposita*, *36*(8), 799–806. https://doi.org/10.1007/s001260100209
Hill, K. C., & Gleadow, A. J. W. (1989). Uplift and thermal history of the Papuan Fold Belt, Papua New Guinea: Apatite fission track analysis. *Australian Journal of Earth Sciences*, *36*(4), 515–539. https://doi.org/10.1080/08120098908729507
Hill, K. C., & Hall, R. (2003). Mesozoic-Cenozoic evolution of Australia's New Guinea margin in a west Pacific context. In *Evolution and dynamics of the Australian plate*. Geological Society of America. https://doi.org/10.1130/0-8137-2372-8.265
Hill, K. C., & Raza, A. (1999). Arc-continent collision in Papua Guinea: Constraints from fission track thermochronology. *Tectonics*, *18*(6), 950–966. https://doi.org/10.1029/1999TC900043
Holm, R. J., Rosenbaum, G., & Richards, S. W. (2016). Post 8 Ma reconstruction of Papua New Guinea and Solomon Islands: Microplate tectonics in a convergent plate boundary setting. *Earth-Science Reviews*, *156*, 66–81. https://doi.org/10.1016/j.earscirev.2016.03.005
Holm, R. J., Spandler, C., & Richards, S. W. (2013). Melanesian arc far-field response to collision of the Ontong Java Plateau: Geochronology and petrogenesis of the Simuku Igneous Complex, New Britain, Papua New Guinea. *Tectonophysics*, *603*, 189–212. https://doi.org/10.1016/j.tecto.2013.05.029
Holm, R. J., Spandler, C., & Richards, S. W. (2015). Continental collision, orogenesis and arc magmatism of the Miocene Maramuni arc, Papua New Guinea. *Gondwana Research*, *28*(3), 1117–1136. https://doi.org/10.1016/j.gr.2014.09.011
Holm, R. J., Tapster, S., Jelsma, H. A., Rosenbaum, G., & Mark, D. F. (2019). Tectonic evolution and copper-gold metallogenesis of the Papua New Guinea and Solomon Islands region. *Ore Geology Reviews*, *104*, 208–226. https://doi.org/10.1016/j.oregeorev.2018.11.007
Jowitt, S. M., & McNulty, B. A. (2021). Battery and energy metals: Future drivers of the minerals industry? *SEG Discovery*, *127*, 11–18. https://doi.org/10.5382/2021-127.fea-01
Larcher, D., & Tarascon, J.-M. (2015). Towards greener and more sustainable batteries for electrical energy storage. *Nature Chemistry*, *7*(1), 19–29. https://doi.org/10.1038/nchem.2085
Lee, C.-T. A., & Tang, M. (2020). How to make porphyry copper deposits. *Earth and Planetary Science Letters*, *529*, 115868. https://doi.org/10.1016/j.epsl.2019.115868
Malinverno, A. (1991). Inverse square-root dependence of mid-ocean-ridge flank roughness on spreading rate. *Nature*, *352*(6330), 58–60. https://doi.org/10.1038/352058a0
Mather, B. R., Müller, R. D., Zahirovic, S., Cannon, J., Chin, M., Ilano, L., et al. (2024). Deep time spatio-temporal data analysis using pyGPlates with Plate Tectonic-Tools and GPlately. *Geoscience Data Journal*, *11*(1), 3–10. https://doi.org/10.1002/gdj3.185
Meinert, L. D. (2007). Mineral deposits of Canada: A synthesis of major deposit types, district metallogeny, the evolution of geological provinces and exploration methods. *Economic Geology*, *102*(7), 1355. https://doi.org/10.2113/gsecongeo.102.7.1355
Merdith, A. S., del Real, P. G., Daniel, I., Andreani, M., Wright, N. M., & Coltice, N. (2020). Pulsated global hydrogen and methane flux at mid-ocean ridges driven by Pangea breakup. *Geochemistry, Geophysics, Geosystems*, *21*(4), e2019GC008869. https://doi.org/10.1029/2019GC008869
Mordelet, F., & Vert, J.-P. (2014). A bagging SVM to learn from positive and unlabeled examples. *Pattern Recognition Letters*, *37*, 201–209. https://doi.org/10.1016/j.patrec.2013.06.010
Mudd, G. M., & Jowitt, S. M. (2018). Growing global copper resources, reserves and production: Discovery is not the only control on supply. *Economic Geology*, *113*(6), 1235–1267. https://doi.org/10.5382/econgeo.2018.4590
Müller, D., Herzig, P. M., Scholten, J. C., & Hunt, S. (2002). Ladolam gold deposit, Lihir Island, Papua New Guinea: Gold mineralization hosted by alkaline rocks. In *Integrated methods for discovery: Global exploration in the twenty-first century*. Society of Economic Geologists. https://doi.org/10.5382/SP.09.16
Müller, R. D., Cannon, J., Qin, X., Watson, R. J., Gurnis, M., Williams, S., et al. (2018). GPlates: Building a virtual Earth through deep time. *Geochemistry, Geophysics, Geosystems*, *19*(7), 2243–2261. https://doi.org/10.1029/2018GC007584
Müller, R. D., & Dutkiewicz, A. (2018). Oceanic crustal carbon cycle drives 26-million-year atmospheric carbon dioxide periodicities. *Science Advances*, *4*(2), eaaq0500. https://doi.org/10.1126/sciadv.aaq0500
Müller, R. D., Mather, B., Dutkiewicz, A., Keller, T., Merdith, A., Gonzalez, C. M., et al. (2022). Evolution of Earth's tectonic carbon conveyor belt. *Nature*, *605*(7911), 629–639. https://doi.org/10.1038/s41586-022-04420-x
Müller, R. D., Seton, M., Zahirovic, S., Williams, S. E., Matthews, K. J., Wright, N. M., et al. (2016). Ocean basin evolution and global-scale plate reorganization events since Pangea breakup. *Annual Review of Earth and Planetary Sciences*, *44*(1), 107–138. https://doi.org/10.1146/annurev-earth-060115-012211
Müller, R. D., Zahirovic, S., Williams, S. E., Cannon, J., Seton, M., Bower, D. J., et al. (2019). A global plate model including lithospheric deformation along major rifts and orogens since the Triassic. *Tectonics*, *38*(6), 1884–1907. https://doi.org/10.1029/2018TC005462
Myers, L., & Sirois, M. J. (2004). Spearman correlation coefficients, differences between. *Encyclopedia of Statistical Sciences*, *12*. https://doi.org/10.1002/0471667196.ess5050.pub2
Nathwani, C. L., Wilkinson, J. J., Brownscombe, W., & John, C. M. (2023). Mineral texture classification using deep convolutional neural networks: An application to zircons from porphyry copper deposits. *Journal of Geophysical Research: Solid Earth*, *128*(2), e2022JB025933. https://doi.org/10.1029/2022JB025933
O'Neill, C., Müller, R. D., & Steinberger, B. (2005). On the uncertainties in hot spot reconstructions and the significance of moving hot spot reference frames. *Geochemistry, Geophysics, Geosystems*, *6*(4), Q04003. https://doi.org/10.1029/2004GC000784
Park, J.-W., Campbell, I. H., Chiaradia, M., Hao, H., & Lee, C.-T. (2021). Crustal magmatic controls on the formation of porphyry copper deposits. *Nature Reviews Earth & Environment*, *2*(8), 542–557. https://doi.org/10.1038/s43017-021-00182-8
Pedregosa, F., Varoquaux, G., Gramfort, A., Michel, V., Thirion, B., Grisel, O., et al. (2011). Scikit-learn: Machine learning in Python. *Journal of Machine Learning Research*, *12*, 2825–2830.

Petterson, M., Babbs, T., Neal, C., Mahoney, J., Saunders, A., Duncan, R., et al. (1999). Geological–tectonic framework of Solomon Islands, SW Pacific: Crustal accretion and growth within an intra-oceanic setting. *Tectonophysics*, *301*(1), 35–60. https://doi.org/10.1016/S0040-1951(98)00214-5
Plunder, A., Thieulot, C., & van Hinsbergen, D. J. J. (2018). The effect of obliquity on temperature in subduction zones: Insights from 3-D numerical modeling. *Solid Earth*, *9*(3), 759–776. https://doi.org/10.5194/se-9-759-2018
Qi, Y., Klein-Seetharaman, J., & Bar-Joseph, Z. (2005). Random forest similarity for protein-protein interaction prediction from multiple sources. In *Biocomputing* (pp. 531–542). https://doi.org/10.1142/9789812702456_0050
Qu, X., Hou, Z., & Li, Y. (2004). Melt components derived from a subducted slab in late orogenic ore-bearing porphyries in the Gangdese copper belt, southern Tibetan plateau. *Lithos*, *74*(3), 131–148. https://doi.org/10.1016/j.lithos.2004.01.003
Richards, J. P. (2003). Tectono-magmatic precursors for porphyry Cu-(Mo-Au) deposit formation. *Economic Geology*, *98*(8), 1515–1533. https://doi.org/10.2113/gsecongeo.98.8.1515
Richards, J. P. (2009). Postsubduction porphyry Cu-Au and epithermal au deposits: Products of remelting of subduction-modified lithosphere. *Geology*, *37*(3), 247–250. https://doi.org/10.1130/G25451A.1
Richards, J. P. (2013). Giant ore deposits formed by optimal alignments and combinations of geological processes. *Nature Geoscience*, *6*(11), 911–916. https://doi.org/10.1038/ngeo1920
Richards, J. P. (2014). Porphyry and related deposits in subduction and post-subduction settings. *Acta Geologica Sinica - English Edition*, *88*(s2), 535–537. https://doi.org/10.1111/1755-6724.12374_19
Richards, S. W., & Holm, R. J. (2013). Tectonic preconditioning and the formation of giant porphyry deposits. In *Tectonics, metallogeny, and discovery: The North American Cordillera and similar accretionary settings*. Society of Economic Geologists. https://doi.org/10.5382/SP.17.08
Rodriguez-Galiano, V., Chica-Olmo, M., & Chica-Rivas, M. (2014). Predictive modelling of gold potential with the integration of multisource information based on random forest: A case study on the Rodalquilar area, Southern Spain. *International Journal of Geographical Information Science*, *28*(7), 1336–1354. https://doi.org/10.1080/13658816.2014.885527
Rodriguez-Galiano, V., Sanchez-Castillo, M., Chica-Olmo, M., & Chica-Rivas, M. (2015). Machine learning predictive models for mineral prospectivity: An evaluation of neural networks, random forest, regression trees and support vector machines. *Ore Geology Reviews*, *71*, 804–818. https://doi.org/10.1016/j.oregeorev.2015.01.001
Rosenbaum, G., Giles, D., Saxon, M., Betts, P. G., Weinberg, R. F., & Duboz, C. (2005). Subduction of the Nazca Ridge and the Inca Plateau: Insights into the formation of ore deposits in Peru. *Earth and Planetary Science Letters*, *239*(1), 18–32. https://doi.org/10.1016/j.epsl.2005.08.003
Rosenbaum, G., & Mo, W. (2011). Tectonic and magmatic responses to the subduction of high bathymetric relief. *Gondwana Research*, *19*(3), 571–582. (Island Arcs: Their role in growth of accretionary orogens and mineral endowment). https://doi.org/10.1016/j.gr.2010.10.007
Sillitoe, R. H. (1972). A plate tectonic model for the origin of porphyry copper deposits. *Economic Geology*, *67*(2), 184–197. https://doi.org/10.2113/gsecongeo.67.2.184
Sillitoe, R. H. (1997). Characteristics and controls of the largest porphyry copper-gold and epithermal gold deposits in the circum-Pacific region. *Australian Journal of Earth Sciences*, *44*(3), 373–388. https://doi.org/10.1080/08120099708728318
Sillitoe, R. H. (2010). Porphyry copper systems. *Economic Geology*, *105*(1), 3–41. https://doi.org/10.2113/gsecongeo.105.1.3
Singh, A., Thakur, N., & Sharma, A. (2016). A review of supervised machine learning algorithms. In *3rd International Conference on Computing for Sustainable Global Development* (pp. 1310–1315).
Sun, T., Chen, F., Zhong, L., Liu, W., & Wang, Y. (2019). GIS-based mineral prospectivity mapping using machine learning methods: A case study from Tongling ore district, eastern China. *Ore Geology Reviews*, *109*, 26–49. https://doi.org/10.1016/j.oregeorev.2019.04.003
Tetley, M. G., Williams, S. E., Gurnis, M., Flament, N., & Müller, R. D. (2019). Constraining absolute plate motions since the Triassic. *Journal of Geophysical Research: Solid Earth*, *124*(7), 7231–7258. https://doi.org/10.1029/2019JB017442
Tosdal, R. M., & Richards, J. P. (2001). Magmatic and structural controls on the development of porphyry Cu ± Mo ± Au deposits. In *Structural controls on ore genesis*. Society of Economic Geologists. https://doi.org/10.5382/Rev.14.06
Tregoning, P., McQueen, H., Lambeck, K., Jackson, R., Little, R., Saunders, S., & Rosa, R. (2000). Present-day crustal motion in Papua New Guinea. *Earth Planets and Space*, *52*(10), 727–730. https://doi.org/10.1186/BF03352272
Wallace, L. M., Stevens, C., Silver, E., McCaffrey, R., Loratung, W., Hasiata, S., et al. (2004). GPS and seismological constraints on active tectonics and arc-continent collision in Papua New Guinea: Implications for mechanics of microplate rotations in a plate boundary zone. *Journal of Geophysical Research*, *109*(B5), B05404. https://doi.org/10.1029/2003JB002481
Whittaker, J. M., Müller, R. D., Roest, W. R., Wessel, P., & Smith, W. H. (2008). How supercontinents and superoceans affect seafloor roughness. *Nature*, *456*(7224), 938–941. https://doi.org/10.1038/nature07573
Wood, A. O. D., & Hedenquist, J. (2019). Mineral exploration: Discovering and defining ore deposits. *SEG Discovery*, *116*, 1–22. https://doi.org/10.5382/Geo-and-Mining-02
Woodhead, J. D., Eggins, S. M., & Johnson, R. W. (1998). Magma genesis in the New Britain island arc: Further insights into melting and mass transfer processes. *Journal of Petrology*, *39*(9), 1641–1668. https://doi.org/10.1093/petroj/39.9.1641
Zahirovic, S., Matthews, K. J., Flament, N., Müller, R. D., Hill, K. C., Seton, M., & Gurnis, M. (2016). Tectonic evolution and deep mantle structure of the eastern Tethys since the latest Jurassic. *Earth-Science Reviews*, *162*, 293–337. https://doi.org/10.1016/j.earscirev.2016.09.005
Zahirovic, S., Seton, M., & Müller, R. D. (2014). The Cretaceous and Cenozoic tectonic evolution of Southeast Asia. *Solid Earth*, *5*(1), 227–273. https://doi.org/10.5194/se-5-227-2014
Zhang, S., Carranza, E. J. M., Xiao, K., Wei, H., Yang, F., Chen, Z., et al. (2022). Mineral prospectivity mapping based on isolation forest and random forest: Implication for the existence of spatial signature of mineralization in outliers. *Natural Resources Research*, *31*(4), 1981–1999. https://doi.org/10.1007/s11053-021-09872-y
Zuo, R., & Carranza, E. J. M. (2011). Support vector machine: A tool for mapping mineral prospectivity. *Computers & Geosciences*, *37*(12), 1967–1975. https://doi.org/10.1016/j.cageo.2010.09.014

Erratum

The originally published version of this article erroneously listed Sara Polanco as the second corresponding author. Ehsan Farahbakhsh is the sole corresponding author. Additionally, the correct version of the movie file S06 has been added to the supporting information. This may be considered the authoritative version of record.